




Review

Advances in the Study of Magnesium Alloys and Their Use in Bone Implant Material

Peixuan Zhi^{1,2,3,†}, Leixin Liu^{1,2,3,†}, Jinke Chang⁴, Chaozong Liu⁴, Qiliang Zhang², Jian Zhou^{1,2}, Ziyu Liu^{1,4,*} and Yubo Fan^{1,*}

¹ Beijing Advanced Innovation Centre for Biomedical Engineering, School of Engineering Medicine, Beihang University, Beijing 100191, China

² Department of Orthopaedic Surgery, Qingdao Municipal Hospital, Qingdao University, Qingdao 266071, China

³ The First Affiliated Hospital and Its National Resident Standardized Training Base, Dalian Medical University, Dalian 116000, China

⁴ Division of Surgery and Interventional Science, Royal National Orthopaedic Hospital, University College London, London HA7 4LP, UK

* Correspondence: liu_ziyu@buaa.edu.cn (Z.L.); yubofan@buaa.edu.cn (Y.F.)

† These authors contributed equally to this work.

Abstract: Magnesium and magnesium alloys have great application potential in the field of orthopaedics. Compared with traditional inorganic nonmetallic materials and medical polymer materials, magnesium alloys have many advantages, such as better strength, toughness, fatigue resistance, and easy processing. Its mechanical properties are suitable and controllable. It can meet the same elastic modulus, cell compatibility, and biodegradability as human cortical bone. There are also some drawbacks for biodegradability, as magnesium and its alloys, with their high degradation rate, can cause insufficient integrity of the mechanical properties. This paper summarises the research on magnesium and its magnesium alloy materials in the field of bone implantation, looking at what magnesium and its magnesium alloys are, the history of magnesium alloys in bone implant materials, the manufacturing of magnesium alloys, the mechanical properties of magnesium alloys, the biocompatibility and clinical applications of magnesium alloys, the shortcomings, and the progress of research in recent years.

Keywords: magnesium alloy; bone implant material; biomechanical properties; biocompatibility; biodegradability



Citation: Zhi, P.; Liu, L.; Chang, J.; Liu, C.; Zhang, Q.; Zhou, J.; Liu, Z.; Fan, Y. Advances in the Study of Magnesium Alloys and Their Use in Bone Implant Material. *Metals* **2022**, *12*, 1500. <https://doi.org/10.3390/met12091500>

Academic Editors: Jianguang Liu and Zhigang Li

Received: 20 July 2022

Accepted: 30 August 2022

Published: 10 September 2022

Publisher's Note: MDPI stays neutral with regard to jurisdictional claims in published maps and institutional affiliations.



Copyright: © 2022 by the authors. Licensee MDPI, Basel, Switzerland. This article is an open access article distributed under the terms and conditions of the Creative Commons Attribution (CC BY) license (<https://creativecommons.org/licenses/by/4.0/>).

1. Introduction

Bone consists of live cells and minerals surrounded by an extracellular matrix (ECM) [1,2]. The surgical treatment of bone injuries has become commonplace, and millions of patients with bone injuries are seen in emergency departments each year due to involvement in strenuous physical activity, social instability, traffic accidents, and extended human lifespans [3–5]. Bone defects are mainly caused by traumatic avulsions, sequelae of bone isolation due to infection, congenital malformations, or tumour resections, leaving us with the great challenge of reconstructive surgery. The need to induce bone regeneration to repair structural bone defects has stimulated the research and development of a large number of bone repair materials [2,6].

Bone repair is a physiological process influenced by a variety of biomechanical, biochemical, cellular, hormonal, and pathological factors. Continuous bone deposition, resorption, and remodelling, as well as an adequate blood supply, promote bone repair [7]. Based on the basic principles of bone tissue healing, different bone repair materials have been developed. Autograft bones have long been considered the gold standard for bone repair materials when replacing damaged or lost bone because they have all the necessary

properties of osteoconductivity, osteogenesis, and osteoconductivity to stimulate new bone growth. However, these autologous grafts are scarce, and secondary surgery adds to the pain experienced by patients. In addition, there may be donor site complications that do not guarantee clinical benefit, and there is a high incidence of associated complications [4,8,9]. A large number of alternative bone repair materials are increasingly being used to replace autograft bone and are marketed as bone substitutes. The most commonly used products are synthetic composites consisting of calcium phosphate (Ca) ceramics, calcium sulphate, bioactive glass, natural materials, and biomaterials [10–15]. However, the clinical performance of these materials has not been satisfactory. For example, some have mechanical properties and clinically show limited osteoinduction [16,17]. Metallic materials are another alternative used to repair or replace diseased or damaged bone tissue. Metal materials that are currently widely used in orthopaedics include stainless steel and titanium alloys because of their mechanical strength and resistance to fractures [18–21]. However, metal ions or particles may be released through corrosion or abrasion, which can trigger an inflammatory response, reduce biocompatibility, and lead to tissue loss. Once the fracture has fully healed, these inert implants also usually need to be removed by invasive secondary surgery. To minimise trauma to patients and reduce healthcare costs, biodegradable implants can be used to replace conventional metal implants and eliminate the need for secondary surgery [22–26].

Magnesium (Mg) alloys have been hailed as revolutionary biodegradable metal materials for orthopaedic applications due to their good biocompatibility, biodegradability, and acceptable mechanical properties [27–30]. As the fourth most abundant cation in the human body, Mg is one of the most essential nutrients in the body, second only to Ca, K, and Na. The normal Mg content in adults is 21–28 g, of which about 53% is found in bones, 27% in muscle tissue, 19% in soft tissues, and a small amount in the blood and organs such as the liver, brain, and kidneys. Mg can catalyse and activate more than 300 enzymes and is an important activator of various enzymes in cellular metabolic activities, participating in various physiological activities such as protein and DNA synthesis, energy storage and transport, nerve signal transmission, and muscle contraction. Mg deficiency may lead to heart arrhythmia, hypertension, ischaemic heart disease, cerebral infarction, osteoporosis, and other diseases. The World Health Organization recommends a daily Mg intake of 280–300 mg for adults and 250 mg for children [31,32]. Therefore, magnesium alloys have a good biosafety basis as biodegradable medical materials. Moreover, magnesium has good osteoinductive properties. Numerous studies have shown that magnesium ions have a role in inducing new bone production. Zhang et al. [33] investigated the osteogenesis of Mg and found that Mg ions stimulated the release of more neurotransmitters (mainly calcitonin gene-related peptide (CGRP)) from sensory nerve terminals in the periosteum, and the increased CGRP further promoted the osteogenic differentiation of stem cells in the periosteum. Figure 1 is a schematic diagram of the mechanism of magnesium ion bone production [33]. The osteoinductive properties of Mg can promote fracture healing, and it is an ideal material for bone repair. Due to the presence of Cl^- in the physiological environment, the magnesium alloy degrades in the body, thus eliminating the need for secondary surgery to remove the implant. Mg^{2+} is a corrosion product of magnesium implants and does not cause unexpected complications, as excess Mg cations are easily eliminated in the urine [34–37]. In addition, magnesium alloys have mechanical properties similar to those of bones. Magnesium alloys are lightweight and have a density ($1.7\text{--}1.9\text{ g/cm}^3$) very similar to that of human cortical bone (1.75 g/cm^3), unlike titanium alloys (Ti-6Al-4V 4.47 g/cm^3) and stainless steel (approx. 7.8 g/cm^3). Compared to the modulus of elasticity of titanium alloys and stainless steel (110 and 200 GPa, respectively), magnesium alloys have a modulus of elasticity of approximately 45 GPa, which is relatively close to that of natural bone at 3–20 GPa, mitigating stress shielding against the significant mechanical mismatch between natural bone and metal implants [38–40]. Thus, magnesium alloys are expected to be biocompatible, biodegradable, lightweight, and load-bearing orthopaedic implants [22,41–43].

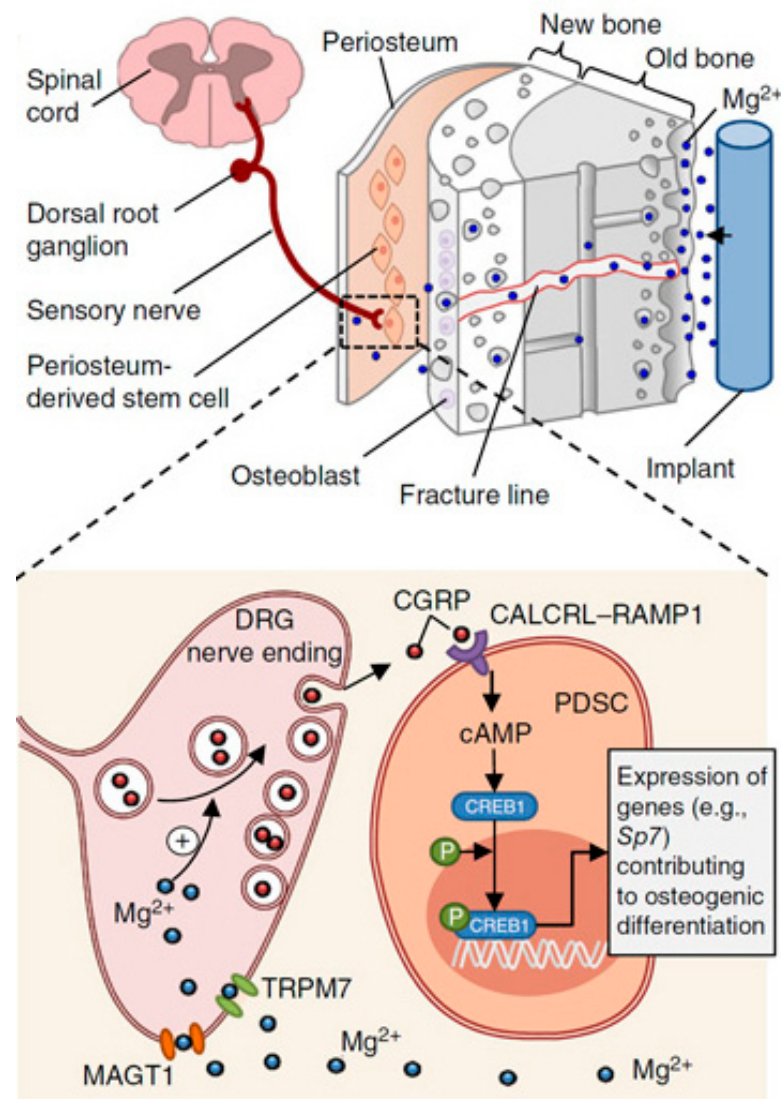


Figure 1. Schematic diagram of the mechanism of magnesium ions for bones [33]. Reprinted with permission from [33]. 2016, Elsevier.

Although significant progress has been made in research into magnesium alloys as bone implants over the past 20 years, the rapid degradation of these materials in the human body remains a major obstacle to their use in the clinic. As a biodegradable material, it is important that the implant degrades at a rate that matches the rate of healing of the bone tissue, which typically includes an early inflammatory phase lasting 3 to 7 days and leading to a remodelling phase lasting approximately 3–4 months, followed by a remodelling phase lasting several months to years [44–46]. Therefore, the implant must remain stable for at least 12 weeks [22]. However, the currently available magnesium alloys degrade too quickly to hold up well during injection. This rapid degradation leads to the formation of hydrogen cavities, rapid loss of the mechanical integrity of the implant, and adverse reactions in the host tissue, such as local swelling and significant pain in the first week after surgery [47,48]. Many opportunities and challenges have recently emerged in the development of magnesium alloys for bone repair. Therefore, it is necessary to summarise the findings of researchers in this field. Compared to recently published reviews [27,49–55], this paper is more focused and specifically discusses biodegradable magnesium alloys for bone repair. We review the fabrication of alloying and the mechanical properties as well as the *in vitro* and *in vivo* biocompatibility of magnesium alloys in bone repair. This is shown in Figure 2.

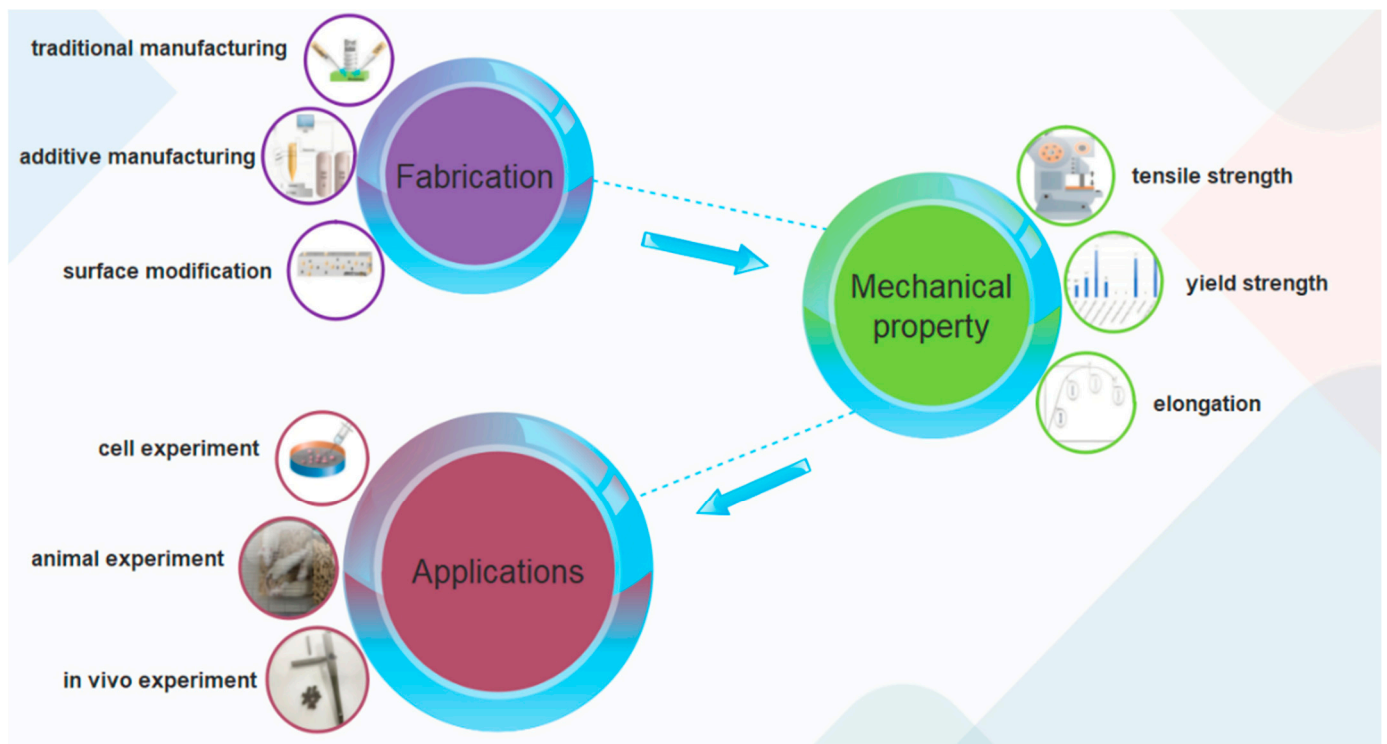


Figure 2. Fabrication, mechanical properties, and in vitro and in vivo biocompatibility of magnesium alloys in bone repair.

2. The Development of Magnesium Alloys and Preparation Processes

2.1. Magnesium Alloy Development

Magnesium alloys have a long history of research as bone repair materials. The first attempt to apply Mg nails, Mg plates, and intramedullary nails to bone repair was made by Payr [1] in 1900. However, no further clinical trials were carried out, as the results of animal studies showed that the degradation of Mg formed a layer of fibrous tissue that prevented further bone healing. In 1906, Lambotte [56] first used magnesium alloys for the clinical internal fixation of fractures, using magnesium plates and steel nails to treat a fracture of the lower leg in a 17-year-old patient. Subsequently, Verbrugge [57] applied the Mg-8Al alloy to 21 fracture operations, and no significant toxicity or irritation was observed. From 1938 to 1945, pure Mg, MgAl-Mn alloy, Mg-10Al alloy, and Mg-Cd alloy were reported for the clinical internal fixation of fractures [58,59]. In one of them, Troitskii and Tsitrin [60] performed 34 procedures using a Mg-Cd alloy and found that Mg promoted bone scab formation, suggesting that the alkaline environment formed during Mg degradation was conducive to osteogenesis. Overall, these early studies all showed that Mg and magnesium alloys were not significantly toxic and could promote bone healing, but the rate of degradation was generally too rapid while not providing effective long-term fixation support [61]. With the widespread use of inert metals such as stainless steel in the field of orthopaedics, magnesium alloy bone repair materials have gradually been fading out of sight. At the end of the 20th century, biodegradable polymer materials and bioactive ceramics began to gain attention for their degradability and good biocompatibility. However, the poor mechanical properties of polymers and ceramics compared to metallic materials severely limit their widespread clinical use. In 2005, the German scholar Witte et al. [62] reintroduced the use of magnesium alloys as a bone repair material. Four magnesium alloys, AZ31, AZ91, WE43, and LAE442, were implanted into the bone marrow cavity of a guinea pig femur. The results at 18 weeks post-operatively showed that LAE442 had the slowest rate of degradation, with a cross-sectional loss of approximately 18% and far more new bone around the magnesium alloy than in the PLA

(Polylactic acid) group, demonstrating good osteoconductivity. Since then, degradable medical magnesium alloys have gradually become a research hotspot. Among others, the German HZG Centre for Materials and Coastal Research has received 5 million EUR in annual funding support for the development of biodegradable medical magnesium alloys since 2007. The NSF (National Science Foundation) invested 18 million USD in 2008 to establish the revolutionary National Engineering Research Center for Medical Metals (ERC-RMB) at North Carolina A&M University for research on new medical metals such as biodegradable magnesium alloys. A large number of new medical magnesium alloys are being developed, including Mg-Ca, Mg-Zn, and Mg-RE systems. Studies have shown that magnesium alloys have good biocompatibility and can induce new bone formation and promote fracture healing. The degradation rate of magnesium alloys is also gradually being controlled through the addition of alloying elements and surface modification techniques. In addition, porous Mg scaffolds have been prepared by laser processing or by using techniques such as powder metallurgy with pore-forming agents, which are expected to be used as bone-defect-filling materials [63,64]. In 2013, MAGNEZIX[®] magnesium hollow compression screws from Syntellix in Germany received the first European CE mark for clinical use (as shown in Figure 3, applied to the correction of foot bunions), mainly for the treatment of hand and foot fractures, as well as for non-union fractures [65–67]. More than 25,000 pieces of the MAGNEZIX[®] range are currently in clinical use. In 2015, the K-MET screw (Mg-Ca alloy) produced by U&I in Korea obtained the approval of the Korea Drug Administration (KFDA) for clinical application. Its clinical observations in the internal fixation of hand fractures have shown good fracture healing and complete screw degradation within 6 to 18 months [68]. In China, Shanghai Jiao Tong University, Peking University, and the Institute of Metals of the Chinese Academy of Sciences have also carried out a large amount of relevant research and have achieved promising results. Among them, Dongguan Yi'an Technology and Zhongshan Hospital of Dalian University have collaborated to apply high-purity Mg screws for the autograft fixation of femoral head necrosis, and hundreds of clinical trials have been conducted [69]. One year after surgery, the screw diameter was reduced by approximately 25%, and the bone density around the screw was significantly increased compared to the control group, with no significant increase in serum Mg content.



Figure 3. Bunion correction surgery.

2.2. Magnesium Alloy Preparation Process

At present, the traditional manufacturing methods of magnesium alloys are commonly used for material reduction manufacturing, including turning, milling, and drilling. The common manufacturing methods are selective laser melting (SLM) and wire arc additive manufacturing (WAAM). The heat source is mainly the laser and arc. The materials required for processing are magnesium alloy powder and wire, respectively.

2.2.1. Reduced Material Manufacturing

Traditional material reduction manufacturing, such as milling, turning, and drilling, is an economic manufacturing technology. Danes [70] and others have simulated and compared low-temperature-assisted manufacturing and the dry turning of the AZ31 magnesium alloy. The research shows that the heat generated in the low-temperature turning process is eliminated faster and effectively (up to 60%), and the surface roughness is reduced (56%) (see Figure 4). This prevents accidental explosions due to excessive temperatures during processing [71]. Bertolini [72] et al. have conducted similar research. Davis and Singh [73] conducted a series of studies on AZ31B and AZ91D, and the research shows that the surface corrosion passivation of turning and milling at low temperature has been improved to some extent. Moreover, Davis and Singh [74] tested three different milling environments (wet, low-temperature, and mixed) and low-temperature treated and untreated milling cutters to mill the AZ31B magnesium alloy. The results show that, in the mixed environment, the surface integrity of magnesium alloy was improved by the milling cutter after the low-temperature treatment. Figure 5 introduces the SEM of the milling passivation layer of the low-temperature milling cutter in different milling environments and mixed environments, as well as the existing elements and the wear of two end milling cutters shown on energy-dispersive X-ray spectroscopy (EDS).

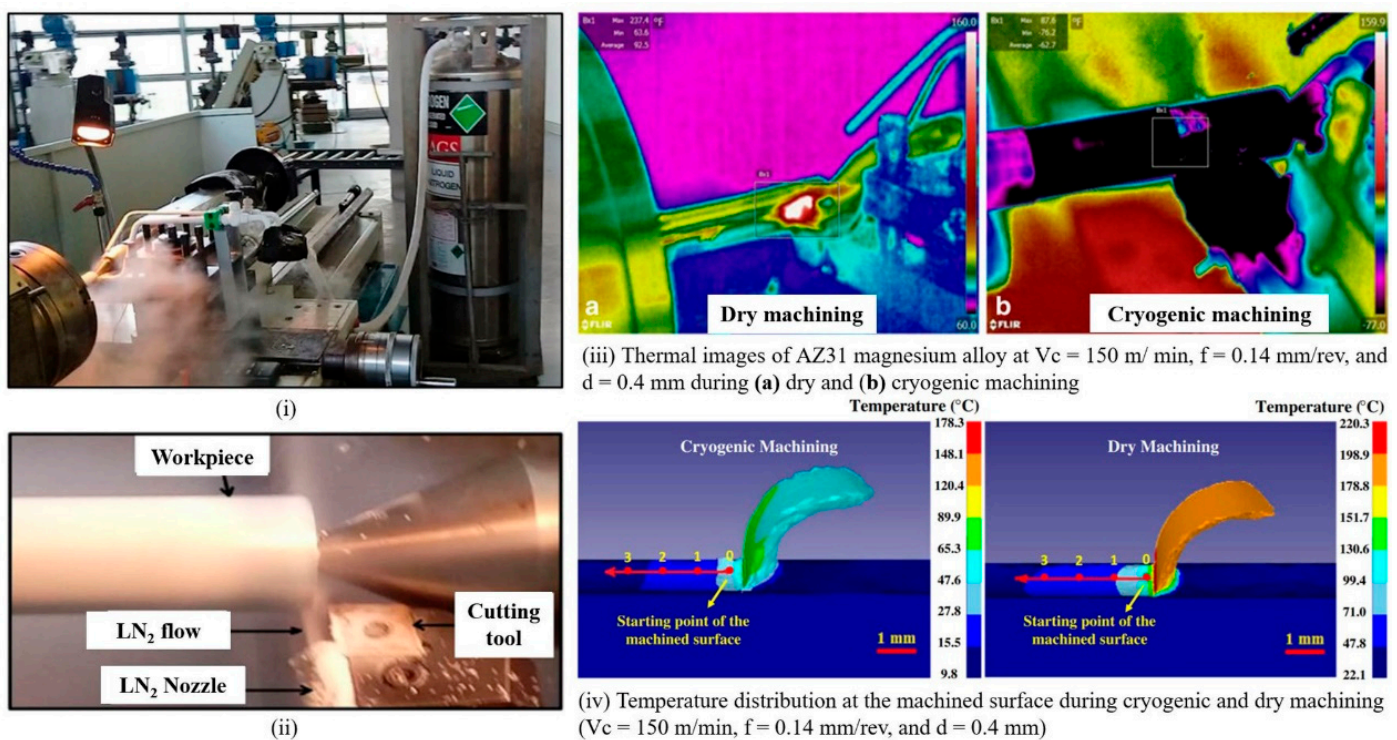


Figure 4. (i) Cryogenic turning setup, (ii) cryogenic turning, (iii) thermal images, and (iv) simulated results of the temperature distribution amid the turning of the Mg alloy AZ31. Reprinted with permission from [70]. 2017, Elsevier.

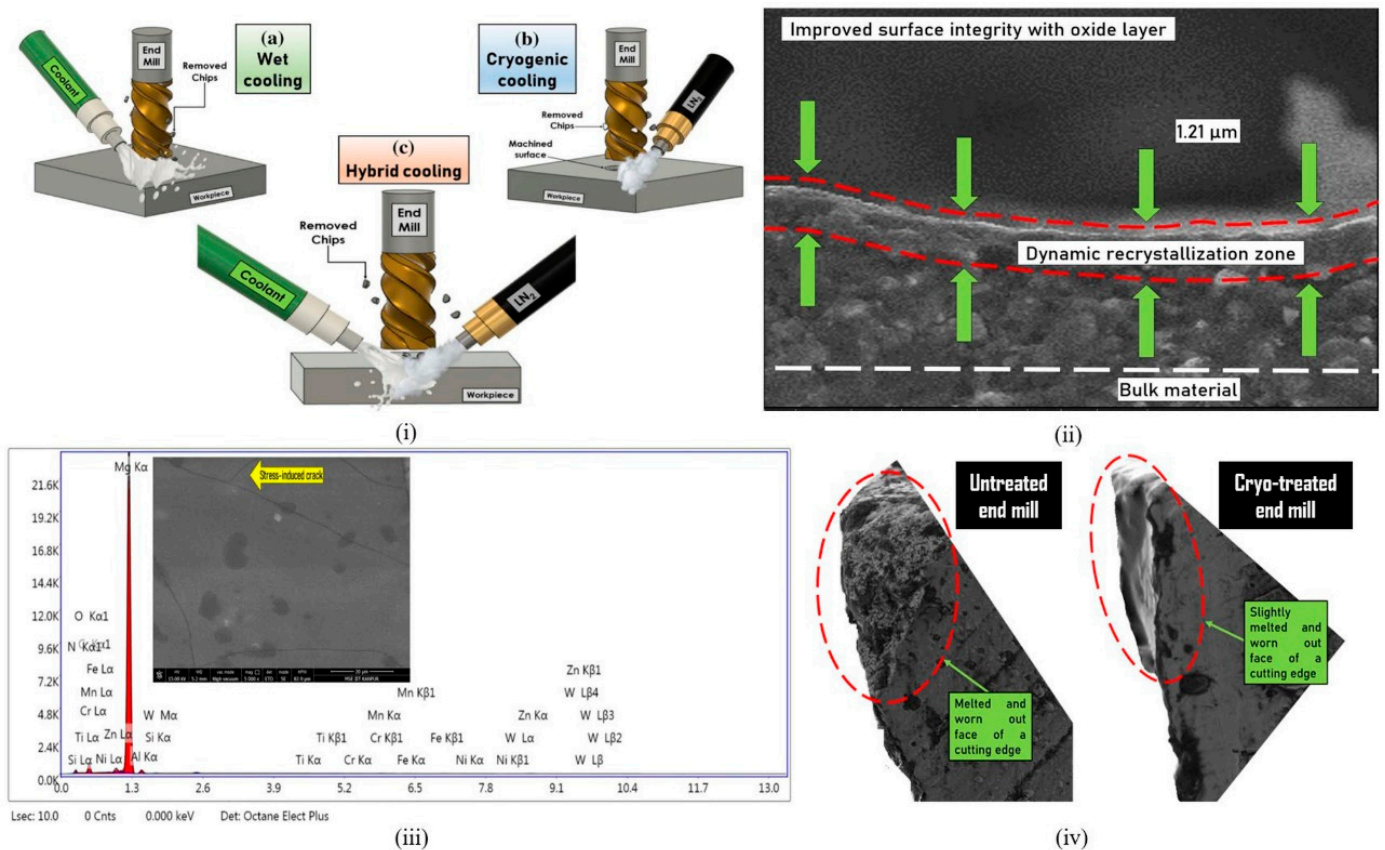


Figure 5. (i) Schematic diagram of three different milling environments of machining Mg alloy AZ31B; (ii) SEM demonstration of the featureless oxide layer on the surface hybrid-milled (wet + cryo) by cryo-treated end mill; (iii) EDS and SEM image of the surface hybrid-milled by cryo-treated end mill; (iv) SEM images displaying tool wear in both the end mills. Reprinted with permission from [74]. 2020, Elsevier.

2.2.2. Additive Manufacturing

Selective laser melting technology uses the laser as the heat source. Its workflow is as follows: The powder is pre-laid on the powder bed first. Then, the heat source, in accordance with the set laser scanning path, melts the powder. After the completion of a table layer, the equipment re-lays the powder, where computer control is used to repeat the operation of the previous layer. Layer-by-layer stacking is used to achieve the additive manufacturing of parts, and the selective laser melting technology equipment schematic diagram is shown in Figure 6 [75]. Selective laser melting, the most commonly used method in additive manufacturing technology today, has several characteristics. (1) It has a smaller spot diameter, hence more concentrated energy input can be generated. It also has the ability to shape small complex parts which are similar to biomedical stents, and improve the surface quality for molding specimens. (2) The low internal stresses generated by the growth process can reduce the residual stresses within the growth specimen and reduce crack generation. (3) The powder requirements are high, and the metal powder requires good flowability in order to improve the uniformity of the spread. The low utilisation of powder in the additive process leads to high additive manufacturing costs, and the quality of the moulding is sensitive to the particle size and shape of the metal powder. (4) The high porosity and low melting and boiling points of magnesium alloys are due to high laser energy input, which can easily cause the oxidation and volatilisation of magnesium elements. This not only affects the composition of the alloy, but it also increases the porosity within the specimen. Although numerous authors have obtained specimens of the AZ91D alloy with a relative density of 99.5% by adjusting the process parameters [76,77], and

although the strength and hardness exceed those of the die-cast AZ91D, it is still difficult to obtain a fully dense metal specimen.

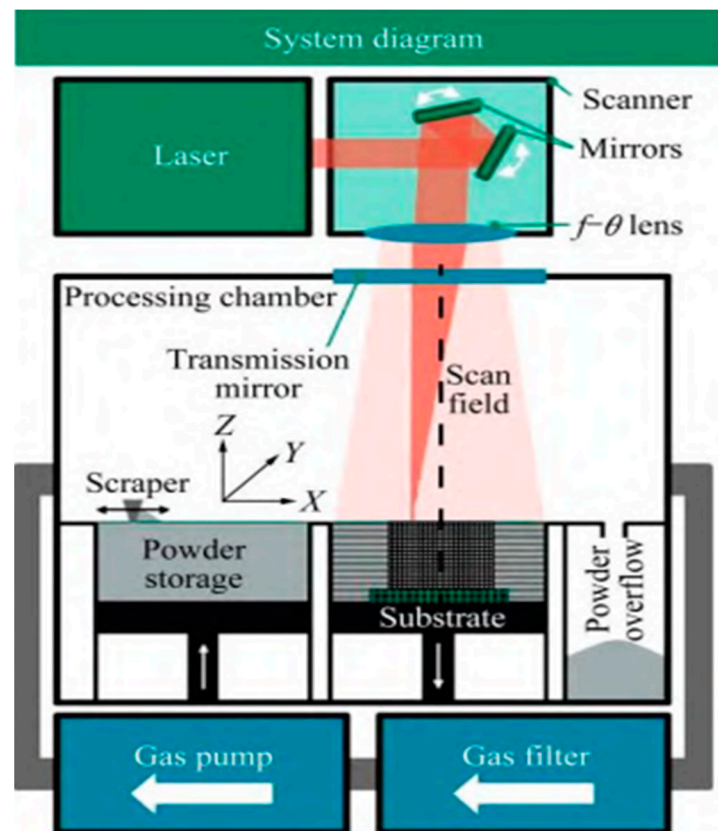


Figure 6. Schematic diagram of selective laser melting machine. Reprinted with permission from [75], 2019, Elsevier.

Wire arc additive manufacturing technology is an additive manufacturing method based on fusion deposition and stacking technology using an electric arc as the heat source and a metal wire as the material that is continuously stacked on top of the original stacked layer, as shown in Figure 7 [78–82]. Commonly used wire arc additive manufacturing methods include gas metal arc welding (GMAW), tungsten-gas-shielded welding (GTAW), and cold metal transition arc welding (CMT) [81]. The deposition rate of GMAW is faster than that of GTAW, but it is prone to smoke and spatter during the welding process, which affects the quality of the specimens. As a cold metal transition technique with minimal energy input, CMT is an arc additive manufacturing method that is suitable for low-melting-point metals and can reduce the oxidation and volatilisation of the metal.

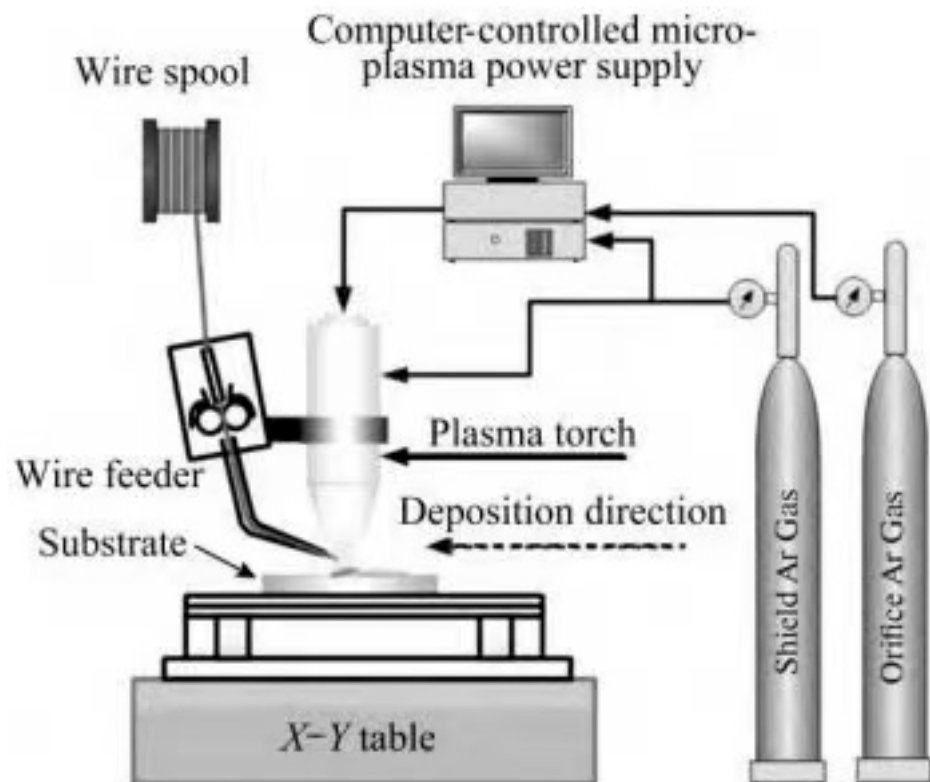


Figure 7. Schematic diagram of wire arc additive manufacturing equipment [82]. Reprinted with permission from [82]. 2018, Elsevier.

Wire arc additive manufacturing technology is characterised by the following. (1) High deposition rate: Wire arc additive manufacturing has the highest stacking rate compared to other additive manufacturing methods, reaching $666 \text{ cm}^3/\text{h}$ with reasonable process parameters [83]. Moreover, wire arc additive manufacturing allows for the machining of large parts and simple processing equipment. (2) High energy efficiency: Comparing different additive manufacturing techniques, laser and powder-based additive manufacturing methods for magnesium alloys have a deposition efficiency of only 14% and an energy efficiency of 20% to 50% [84,85]. The main reason is that the powder has a certain reflection effect on the energy beam and that the unmelted powder around the melt pool is also affected by the heat source. In contrast, wire arc additive manufacturing technology based on filaments and arcs can reach 100% deposition efficiency and 54% to 88% energy efficiency [86,87]. (3) Poor quality of formed parts: Wire arc additive manufacturing has a large melt pool size, high molten metal temperature, and high fluidity. This results in poor surface quality on the sides of the specimen, low specimen forming accuracy compared to laser additive manufacturing, and difficulty in precision machining. Arc additive parts cannot be applied directly and must be post-treated for arc additive specimens. As additive manufacturing technologies mature, additive manufacturing technologies for magnesium alloy materials are also being developed. For example, in response to the problems of volatile and oxidisable magnesium elements and poor molding quality, researchers have proposed the use of high-pressure chambers for laser additive manufacturing [88]. The high pressure applied to the working area increases the evaporation temperature of the magnesium, thereby inhibiting its evaporation. However, due to the size of the high-pressure chamber, only small parts can be processed, and the active nature of magnesium makes additive manufacturing in high-pressure chambers very dangerous. Shen et al. [89] investigated the effect of the GMAW–GTAW composite additive manufacturing method on the properties of the AZ31B alloy by using an experimental method. By regulating the process parameters, the final obtained additive manufactured magnesium alloy was of good qual-

ity and proved that GMAW–GTAW is a suitable method for the additive manufacturing of magnesium alloys.

2.3. Magnesium Alloy Material Surface Modification Technology

Surface modification is a common means of improving the performance of medical magnesium alloys. By preparing a suitable coating on the surface of the magnesium alloy, this not only effectively reduces its corrosion rate, but it also improves the biocompatibility of the surface. Commonly used surface modification methods for medical magnesium alloys include chemical conversion, micro-arc oxidation or anodic oxidation, electrochemical deposition, bionic deposition, the sol-gel method, ion injection, and the lifting and spin coating methods applied to polymer coatings. The various surface modification methods are summarised separately below (Table 1).

2.3.1. Chemical Conversion Method

Chemical transformation methods are used to form a film layer on the surface of the sample through chemical reactions, mainly including fluorination and alkali heat treatment. The fluorination treatment involves immersing the magnesium alloy sample in a 40% HF solution for various times to form a dense MgF_2 film layer on the surface of the magnesium alloy. The thickness of the film layer depends on the time of immersion and is typically a few microns. Chiu et al. [90] prepared a 1.5 mm-thick MgF_2 film layer on the surface by immersing pure Mg in a HF solution for 48 h. Electrochemical tests showed that the self-corrosion current density of the treated sample was reduced to 1/40th of the original. Witte et al. [91] first immersed LAE442 samples in a NaOH solution to form a $\text{Mg}(\text{OH})_2$ film layer on the surface and then immersed them in a HF solution for 96 h to convert them to a MgF_2 film layer of 150–200 nm thickness. The samples were implanted into the femoral condyles of rabbits, and the results show that the coating reduced the corrosion rate of the magnesium alloy to some extent but increased localised corrosion. Overall, the fluorination process is simple and inexpensive, and the coating bonds well to the substrate. However, due to the thin MgF_2 film layer, its protective effect on the magnesium matrix is limited. In addition, fluorination is often used as a pretreatment process for other coatings [92]. The alkali heat treatment involves immersing the sample in an alkaline solution such as NaOH or NaHCO_3 for a period of time, followed by a heat treatment, resulting in a tens-of-microns-thick layer of $\text{Mg}(\text{OH})_2$, MgO, or MgCO_3 . The alkali heat treatment process is simple, the coating is biocompatible, and it can protect the magnesium alloy substrate to some extent. Gu et al. [44] treated Mg-1Ca by immersion in Na_2HPO_4 , Na_2CO_3 , and NaHCO_3 solutions for 24 h, followed by holding at 773 K for 12 h. The soaking results show that all three treatments significantly reduced the corrosion rate of Mg-1Ca, in the following descending order: Na_2CO_3 group > Na_2HPO_4 group > NaHCO_3 group. Maurya et al. [93] showed by this method that, in a 3.5% aqueous solution of NaCl, the corrosion current densities of the PCC-coated LAT971 and LATZ9531 alloys were 6.74×10^{-7} mA/cm² and 5.39×10^{-7} mA/cm² respectively, well below the uncoated LAT971 (0.82 mA/cm²) and LATZ9531 (0.34 mA/cm²), with a corrosion protection efficiency of 99%, as shown in Figure 8.

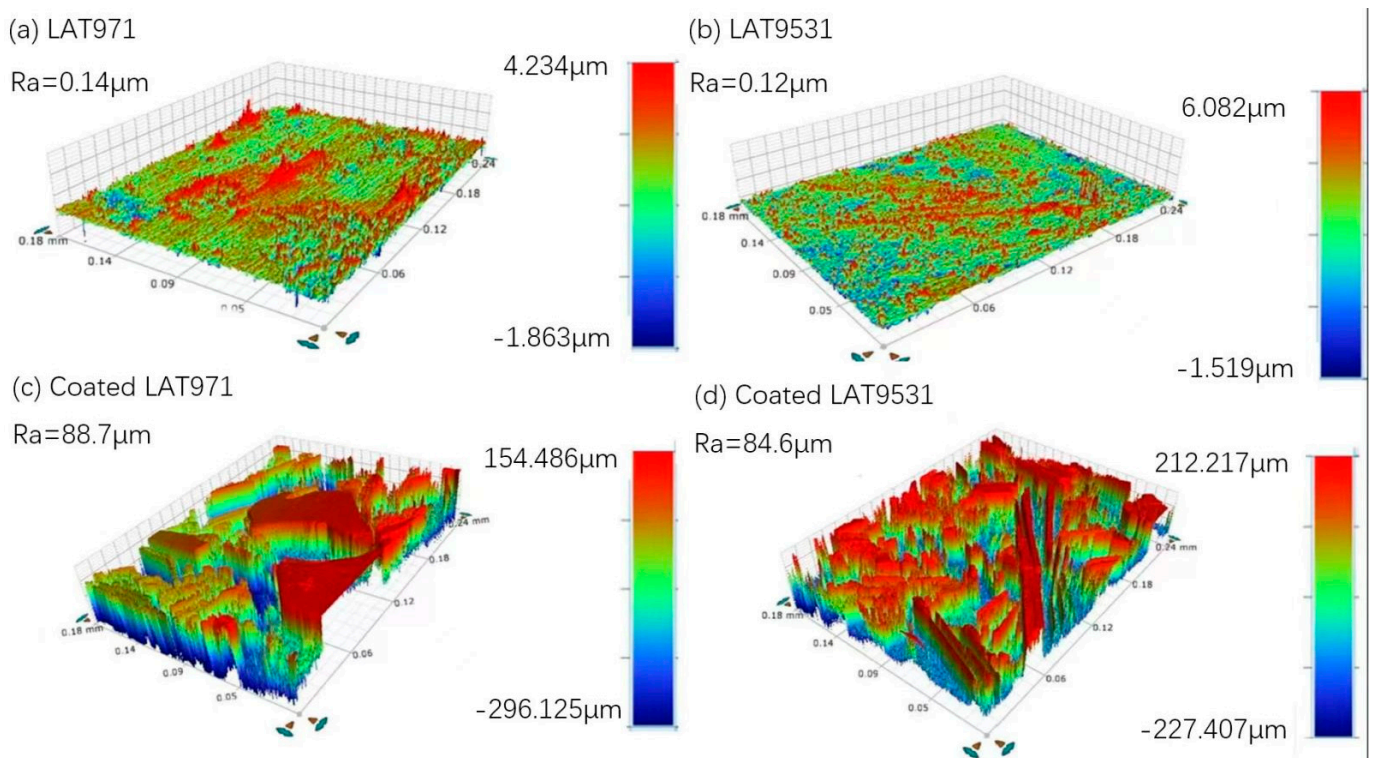


Figure 8. Surface profiling of uncoated (a,b) and PCC-coated (c,d) LAT971 and LAT9531 alloys, respectively [93]. Reprinted with permission from [93]. 2018, Elsevier.

2.3.2. Anodic and Micro-Arc Oxidation Methods

Anodising is the process whereby a magnesium alloy is placed as an anode in a suitable electrolyte, and an oxide film is formed on the surface of the sample by loading it with a certain amount of current. Micro-arc oxidation (MAO) is a modification of the anodic oxidation method, which involves the formation of an oxide-based film layer on the surface of magnesium alloys by arc discharge at high temperatures in an electrolyte and at a certain voltage [94]. The coatings obtained by these two processes have the advantages of high hardness, good bonding, and good biocompatibility. However, the method is complex, the coating is mostly defective and brittle, and some of the coating does not degrade easily. Gu et al. [95] subjected Mg-1Ca alloy to micro-arc oxidation and found that the thickness of the film and pore structure could be modulated by varying the voltage, thus affecting the corrosion rate of the sample. Gao et al. [96] prepared nano-HA by micro-arc oxidation on a Mg-Zn-Ca alloy, which has twice the binding strength compared to electrochemical deposited coatings and can effectively reduce the corrosion rate of the alloy. Cui et al. [97] studied the factors influencing the corrosion of micro-arc oxidised Mg-Ca alloys. The results show that the corrosion rate of the MAO-coated Mg-Ca alloy is mainly related to the corrosion resistance of the substrate, the porosity of the coating, and the electric coupling effect between the coating and the substrate, and the coating thickness has no significant effect on the corrosion resistance of the coating. Figure 9 shows that through-holes and micro-cracks in the MAO coating are the main contributors to the electrochemical corrosion of the magnesium–calcium alloy substrate. As the number of through-holes increases, the galvanic corrosion effect becomes more severe, resulting in higher degradation rates.

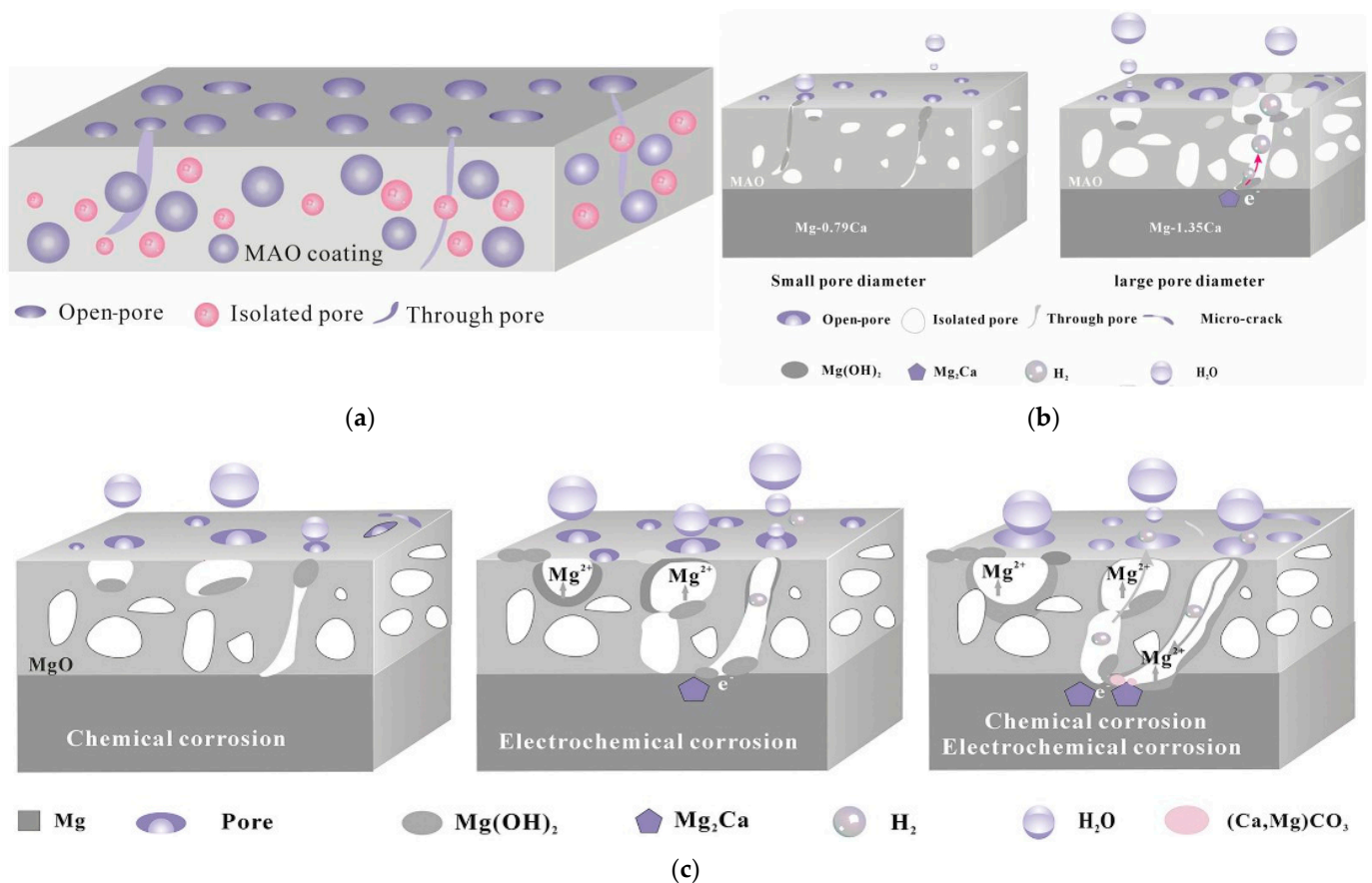


Figure 9. (a) Schematic illustration of the various pores in the MAO coatings on Mg alloys; (b) Schematic illustrations of the influence of pore diameter on corrosion; (c) Schematic illustrations of the chemical degradation [97]. Reprinted with permission from [97]. 2017, Elsevier.

2.3.3. Electrochemical Deposition Method

Electrochemical deposition is the deposition of ions from a solution onto the surface of a sample under the action of an electric field. By varying parameters such as current, voltage, electrolyte concentration and pH, the thickness and organisation of the coating can be regulated. Its coating composition is generally calcium and phosphorus salts, which are biocompatible, but the coating bond is average. Wang et al. [98] prepared calcium-deficient HA coatings on Mg-Zn-Ca surfaces by a pulsed electrodeposition method with significantly improved coating bonding. Song et al. [99] prepared three coatings of fluorinated hydroxyapatite (FHA), HA, and perovskite (DCPD) on a Mg-Zn alloy and found that the corrosion resistance of FHA and HA was better than that of the DCPD coating.

2.3.4. Bionic Deposition Method

The bionic deposition method involves immersing a magnesium alloy sample in a suitable solution to deposit calcium and phosphorus salts on the surface of the sample. It is a simple process with good biocompatibility but poor binding. Keim et al. [100] and Zhang et al. [101] prepared calcium and phosphate coatings on the surface of the samples by immersing pure Mg in simulated body fluid (SBF), respectively, and showed that the coatings slowed down the corrosion of pure Mg and facilitated the growth of cell adhesion. Gray-Munro et al. [102] concluded that solutions that are more acidic are more suitable for the deposition of calcium and phosphorus salts on the surface of magnesium alloys. Wang et al. [103] immersed AZ31B in an electrolyte at pH 4 for 24 h and successfully prepared a calcium-phosphorus coating that was about 20 μm -thick and that showed good corrosion resistance and biocompatibility.

2.3.5. Sol-Gel Method

The sol-gel method uses a colloidal solution as a precursor to polymerise on the surface of the magnesium alloy to form a three-dimensional mesh-like gel, which is then dried and cured to finally form a coating. Its coatings are biocompatible but have average binding power. Hu et al. [104] prepared a layer of a nano-TiO₂ coating on the surface of an AZ31 magnesium alloy by the sol-gel method and found that the coating particle size and degradation rate increased with increasing curing annealing temperature. Roy et al. [105] prepared approximately 50 µm-thick porous Si-containing calcium and phosphorus coatings on Mg-4Y samples by the gel-solution method and found that Si promoted the crystallisation of HA.

2.3.6. Ion Injection Method

The ion injection method involves injecting high-energy ions into the surface of the sample to form compounds that improve the hardness, wear resistance, corrosion resistance, etc., of the surface. Its coating thickness is generally less than 1 µm, it is firmly bonded to the substrate, the elements are selectable, and the process can be controlled. The elements commonly used today are Ti, Zn, N, and Zr. Wan et al. [106] injected Zn into the surface of a Mg-Ca alloy and found that the surface hardness of the sample increased significantly, whereas the corrosion rate decreased. Wu et al. [107] injected N and Ti ions onto the surface of AZ31 samples, respectively, and found that the N-treated samples had better corrosion resistance.

2.3.7. Polymer Coating

The main polymer coatings are polycaprolactone (PCL), poly(L-lactic acid) (PLLA), poly(lactic acid)-hydroxyacetic acid copolymer (PLGA), chitosan, etc. They are generally prepared by the Dip and Lift method and the spin coating method. The disadvantages are the acidic nature of the degradation products, which can cause inflammation, and the poor abrasion resistance of the coating. The mass of a polymer coating is generally determined by the molecular weight of the solute and the concentration of the solution. Li et al. [108] prepared PLGA coatings on Mg-6Zn samples by lifting and found that the thickness of the coatings prepared in a 4% solution ((72 ± 5) µm) was much greater than those prepared in a 2% solution ((33 ± 5) µm), but the difference in corrosion resistance between the two was not significant [109].

Table 1. Common surface modification techniques and their characteristics.

Classification		Features	References
Chemical conversion method	Fluoridation	Simple process, low cost, and good bonding of the coating to the substrate, but can increase localised corrosion.	[90]
	Alkali heat treatment	Simple process, good biocompatibility of the coating, and a certain degree of protection of the magnesium alloy substrate.	
Anodising and micro-arc oxidation	Anodising	High hardness, good bonding, and good biocompatibility. However, the method is complex, the coatings are mostly defective and brittle, and some of them do not degrade easily.	[95]
	Micro-arc oxidation (MAO)		
Electrochemical deposition		Good biocompatibility, but average coating adhesion.	[98]

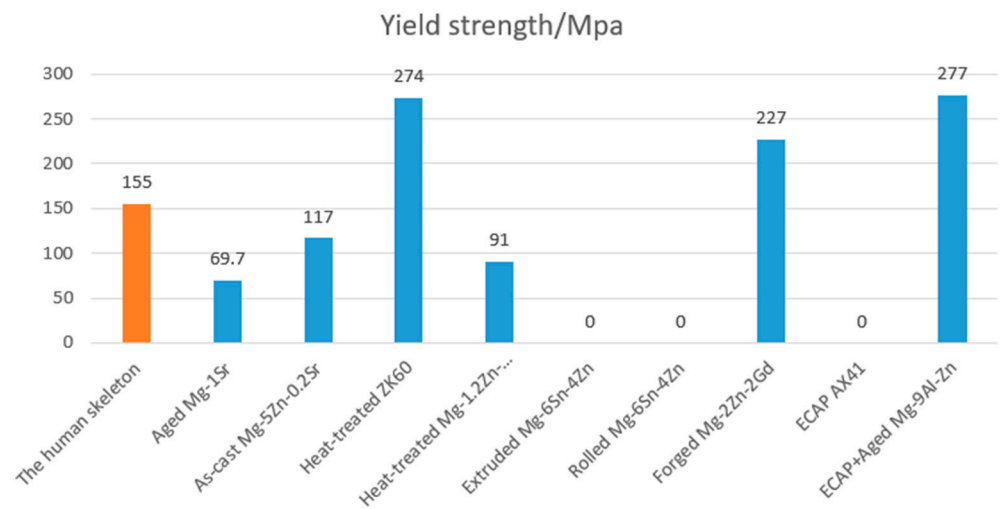
Table 1. Cont.

Classification		Features	References
Bionic deposition method		It is a simple process with good biocompatibility but has poor binding power.	[101]
Sol-gel method		Improves surface hardness, wear resistance, and corrosion resistance.	[104]
Ion injection method		Improves surface hardness, wear resistance, and corrosion resistance.	[106]
Polymer coatings	Dip and Lift Method	It is relatively homogeneous and dense, has a controlled composition thickness, and is available for subsequent drug loading. The disadvantage is that the degradation products are acidic and inflammatory, and the coating is less wear-resistant.	[108]
	Spin coating method		

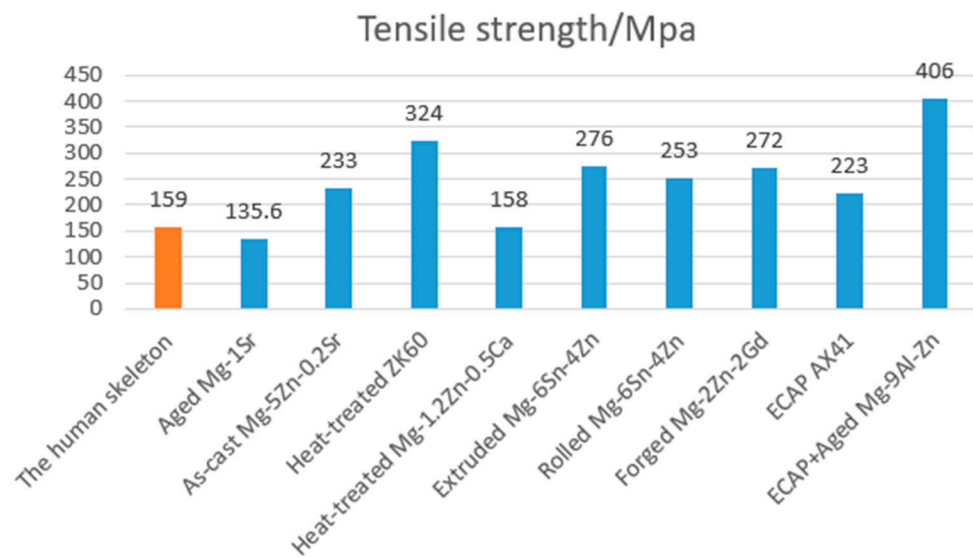
3. Mechanical Properties of Magnesium Alloys

3.1. A Study of the Modulus of Elasticity

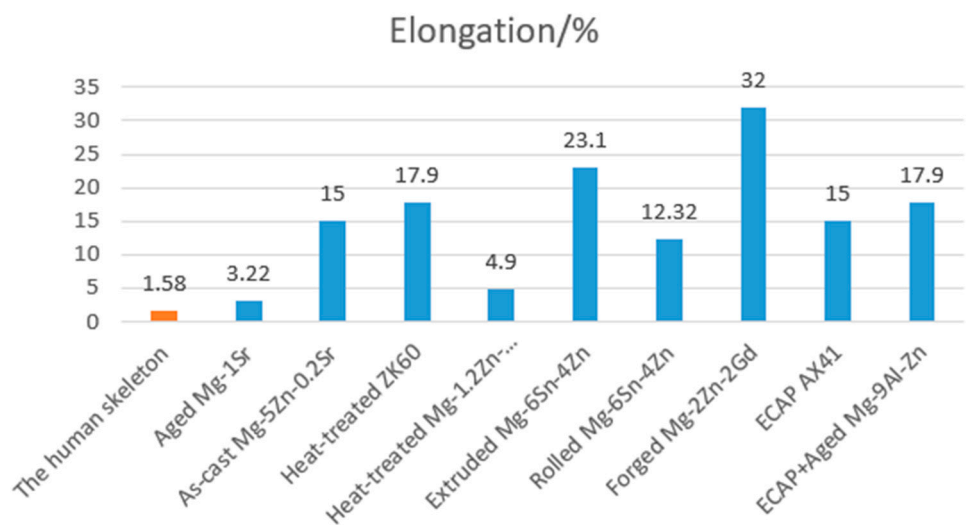
By changing the percentage of alloying elements, the microstructure of the alloy is changed, which in turn affects the mechanical properties of the alloy, resulting in magnesium alloys with excellent overall properties. Wang et al. [110] investigated the effect of the variation of Sr content in Mg-Sr binary alloys on the mechanical properties. Among the three contents of 0.5 wt%, 1 wt%, and 2 wt%, the cast Mg-Sr binary alloy with a content of 1wt% had the best mechanical properties. Its tensile strength, yield strength, and elongation were 92.67 MPa, 56.0 MPa, and 1.27%, respectively, and the properties were not very satisfactory. Under the same process conditions, the alloy with a Sr content of 0.2 wt% has optimum properties, at which point the tensile strength, yield strength, and elongation are 233 MPa, 117 MPa, and 15%, respectively [111]. Heat treatment is also a way of increasing the strength of magnesium alloys. Maier et al. [112] found that the yield strength of the Mg-Y-Nd alloy after T6 heat treatment was 133.3 MPa, the tensile strength was 235.5 MPa, and the elongation was 15.4%. The yield strength of 108.7 MPa, tensile strength of 237.7 MPa, and elongation of 19.2% were all changed compared to the alloy before the heat treatment, mainly due to the precipitation of the second phase, which increased the strength of the matrix. Chen et al. [113] compared the ZK60 alloy in the as-cast, T5 (170 °C, 10 h) heat-treated, and T6 (500 °C, 2 h, air-cooled, and then treated at 170 °C for 10 h) heat-treated states, and the microscopic results showed that the alloy in the T5 state had a small and homogeneous second phase, and therefore it had the best mechanical properties and corrosion resistance. Plastic deformation is another method of processing magnesium alloys, and extrusion deformation is the predominant deformation method for magnesium alloys. Mahallawy et al. [114] extruded a Mg-6Sn-4Zn alloy at an extrusion temperature of 350 °C and an extrusion ratio of 40:1 and obtained grain sizes of 11–13 µm, tensile strengths of 276 MPa, and an elongation of 23.1%. Forging is also often used to improve the mechanical properties of magnesium alloys. Li et al. [115] subjected an annealed Mg-2Zn-2Gd alloy to multiaxial forging and obtained a grain size of (416 ± 140) nm. The alloy had a yield strength of 227 MPa, a tensile strength of 272 MPa, and an elongation of 32%, with excellent strong plasticity matching. In recent years, equal-channel angular extrusion (ECAE) has been an effective method of grain refinement. Krajčák et al. [116] found that the average grain size of an AX41 magnesium alloy with ECAP after eight passes of the type A processing method reached 220 nm, with a maximum strength of 223 MPa, an increase of 30% compared to the extruded state, and the elongation of all samples was higher than 15% at room temperature, with a large amount of dislocation slip and strong grain refinement causing the high strength and elongation. Current research has shown that the strength and plasticity of magnesium alloys can be significantly improved by alloying, heat treatment, and plastic deformation, often by using two or a combination of these three methods, and much research has been conducted in this area (as shown in Figure 10).



(a)



(b)



(c)

Figure 10. (a) Comparison of the yield strength of individual magnesium alloys (the mean of 0 is not

mentioned in the references); (b) Comparison of the tensile strength of individual magnesium alloys; (c) Comparison of the elongation of individual magnesium alloys.

3.2. Frictional Wear Properties of Magnesium Alloys

3.2.1. Frictional Wear of Mg-Al-Zn Alloys

Mg-Al-Zn alloys are widely used, and relatively more research has been conducted on friction and wear properties [117–125], mainly on Mg-3Al-1Zn (AZ31), Mg-9Al-1Zn (AZ91), etc. The addition of Al and Zn not only refines the grain, but it also forms a reticulated $Mg_{17}Al_{12}$ phase, thus improving the mechanical properties and wear resistance of the material. Studies have shown [117] that, under the same conditions, the coefficient of friction and wear rate of the AZ31 alloy are much lower than those of pure magnesium. Das et al. [118] studied the microstructural evolution of AZ31 alloy at high temperatures and found that, at 673 K, the material transferred to the counter-abrasive surface underwent violent deformation and partial recrystallisation. Dynamic recrystallisation and grain growth occurred in the subsurface grains of the contact surfaces due to large plastic deformation, and the plastic strain reached 100% for subsurfaces up to 10 μm and even 300% for surfaces up to 5 μm . This phenomenon is also consistent with the superplastic deformation behaviour of AZ31 at the same temperature. Surface damage and material transfer occur continuously, resulting in a dynamic equilibrium in the friction process and a constant wear rate. Zafari et al. [119,120] investigated the wear mechanism of the AZ91 magnesium alloy under different loading and sliding speed conditions. Chen et al. [121] also investigated the wear mechanism of the AZ91 magnesium alloy and classified the wear into minor and severe wear (Figure 11). Minor wear is subdivided into oxidation wear and spalling wear, and severe wear can also be subdivided into plastic deformation and melting wear. The experimental results summarise the relationship between load and velocity and surface temperature, showing that the transition from light wear to severe wear depends on a certain critical surface temperature. In the case of the AZ91 alloy, severe wear occurs when the surface contact temperature is above 347 K. Other studies [126] have shown that the wear rate of the AZ91D alloy at low loads decreases with increasing temperature (25–200 °C). The reason for this may be that, at higher temperatures, an oxide layer is produced on the friction surface, preventing direct contact between the metals, so the wear rate is reduced. Wang et al. [122] showed that high temperatures increased the thickness of the mechanical mixed layer, which had a hardness of 110–120 HV, greater than the alloy hardness of 80–90 HV, thus alleviating wear. The same phenomenon was found in the AM60 alloy [127]. This shows that, below the critical temperature, the effect of temperature on frictional wear is not the same as at high temperatures.

3.2.2. Frictional Wear of Mg-Al-Si Alloys

The Mg-Al-Si alloy is one of the most heat-resistant magnesium alloys. The strengthening phase Mg_2Si in Mg-Al-Si alloys has a high melting point (1085 °C), a high modulus of elasticity (120 GPa), and a low coefficient of thermal expansion ($7.5 \times 10^{-6} K^{-1}$), thus greatly improving the properties of the material [128,129]. Studies on the AS21 (2.0% Al, 0.70% Si, 0.20% Zn, 0.36% Mn, Mg residual) alloy have pointed out that the wear resistance of the AS21 alloy at room temperature was not as good as that of the AZ91D alloy, mainly because the Vickers hardness of the AS21 alloy was 60.24, which was not as high as that of AZ91D (83.7) [130].

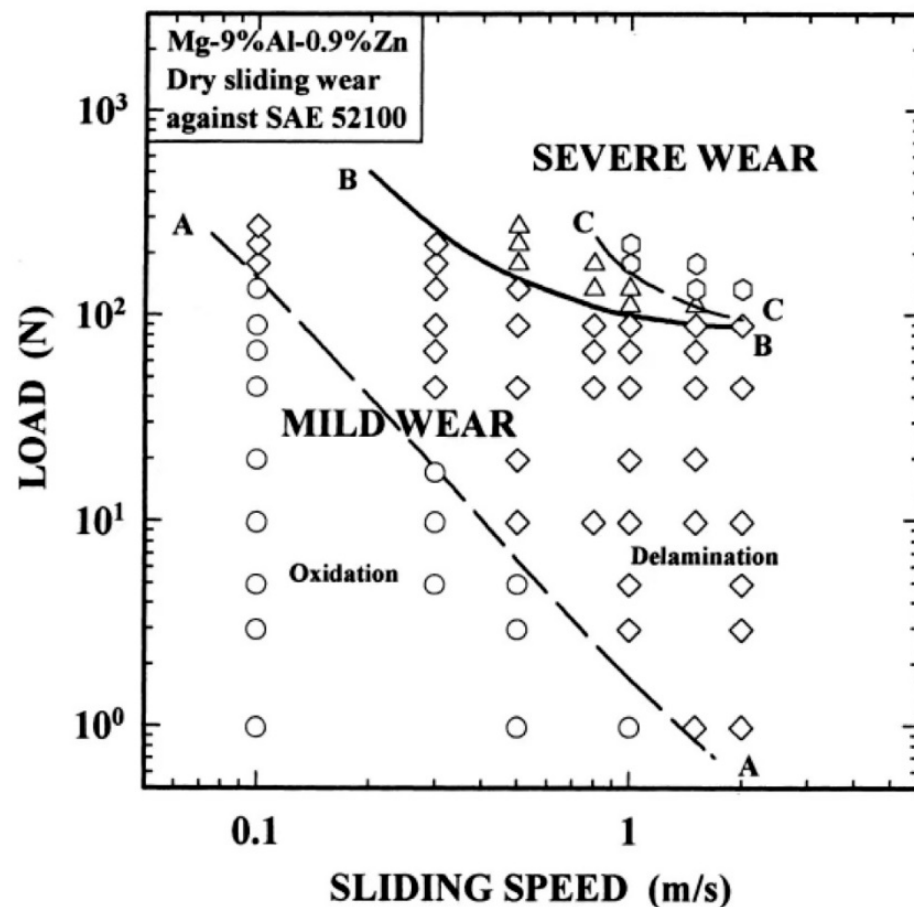


Figure 11. Wear transition map for AZ91 showing the region of dominance of wear mechanisms and the transition boundaries between them; BB: mild wear to severe wear transition; AA: transition between the oxidational wear (\circ) and delamination (\diamond) wear in the mild wear regime; CC: transition between severe deformation induced wear (\triangle) and melt wear (\circ) [121]. Reprinted with permission from [121]. 2000, Elsevier.

3.2.3. Frictional Wear of Mg-Al-Ca and Mg-Zn-Zr Alloys

The Mg-5Al-3Ca-0.12Sr (AXJ530) alloy developed by General Motors has good tensile properties, creep resistance, corrosion resistance, and casting properties, and it is comparable in cost to the AZ91D alloy, with a yield strength of 196 MPa at 175 °C, close to the A380 (3.0–4.0% Cu, 7.5–9.5% Si, 0–1% Mg, 0–2.0% Fe, 0–3.0% Zn, 0–0.5% Mn, 0–0.5% Ni, 0–0.35% Sn, Al balance) aluminium alloy. The study of the frictional wear properties of this alloy is of great relevance due to the high melting point and good thermal stability of the Al_{12}Ca , Mg_2Ca , or $(\text{Mg},\text{Al})_2\text{Ca}$ reinforced phases of the alloy. Hu et al. [131] studied five different AXJ casting alloys with different grain sizes and found that as the grain size within a certain range becomes smaller, the wear resistance becomes higher. For example, under the same friction conditions, the wear rate of an alloy with a grain size of 54.8 μm is greater than that of an alloy with a grain size of 32.3 μm . The reason for this is that, as the grain size becomes smaller, the mechanical properties and hardness become higher, which improves wear resistance. For example, the strength and elongation of AXJ alloys obtained using high-pressure casting with a grain size of 4.5 μm are significantly higher than those of ordinary cast alloys, but the wear resistance is not as high as when the grain size is 32.3 μm [131]. Another similar study [132] showed that the wear properties of ZK60 (Mg-6Zn-0.6Zr) decreased with decreasing grain size at very small grain sizes. It shows that wear resistance is related to grain size. When the grain size is small, the coefficient of friction increases due to the influence of adhesive wear. The friction surface is subjected to large plastic deformation, and the wear rate increases. Conversely, alloys with larger grains

have a wear mechanism of abrasive wear, rather than plastic deformation, and therefore have improved wear properties. Due to the transition from adhesive wear to abrasive wear, the wear resistance of high-pressure-cast AXJ gold is lower than that of ordinary cast alloys. However, the wear rate of the ZK60 alloy grain size of a 100 μ m sample is still less than that of a 40 μ m grain sample, and this result is not the same as AXJ gold. It can be seen that fine grain strengthening can improve the wear resistance of the alloy to some extent, but the wear resistance of magnesium alloys with particularly fine grains is not necessarily good. There are not many relevant studies yet, and more experimental data are needed to prove it.

3.2.4. Frictional Wear of Rare Earth Magnesium Alloys

Because rare earth elements have the advantages of improving the heat resistance of magnesium alloys, refining grain size, and improving casting properties, the application in magnesium alloys has gradually increased in recent years, and many scholars have also been involved in research on the frictional wear properties of rare earth magnesium alloys [133–135]. A systematic study on the frictional wear of Mg-3.85Zn-1.27Ce-0.53Zr (ZE41A) magnesium alloy was conducted in [136,137], and the results show that the coefficient of friction decreases with increasing load and sliding speed, and the wear rate increases with increasing load and sliding speed. There is a gradual increase in the wear rate with increasing load in the slight wear regime and a sharp increase in the wear rate above a certain critical load. At different loads and sliding speeds, the main wear mechanisms are divided into five categories: abrasive wear, oxidation wear, spalling wear, plastic deformation, and melt wear. The wear mechanism of the ZE41A alloy can be controlled by the load and sliding speed. The findings are the same as those for the Mg-Al-Zn alloy, and the friction coefficient varies with friction conditions in the same way as for the Mg-Al-Si alloy. Hu et al. [138,139] studied the wear of two heat-resistant magnesium alloys, Mg-10Gd-3Y-0.4Zr (GW103K) and Mg-11Y-5Gd-2Zn (WGZ1152), under the conditions of a load of 3–15 N, a speed of 0.03–0.24 m/s, and a temperature of 25–200 °C. The counter-wear substrate was a 6 mm-diameter AISI52100 steel ball. The comparison with the AC8A (11.3% Si, 0.81% Mg, 1.25% Cu, 1.34% Ni, Al balance) aluminium alloy was carried out, and it was found that the WGZ1152 alloy had the best wear resistance under dry friction conditions, followed by the GW103K alloy. The wear resistance of the WGZ1152 alloy was found to be the best under dry friction conditions, followed by the GW103K alloy, and the wear rate of both magnesium alloys changed very little with increasing temperature, whereas the dry friction wear rate of the AC8A aluminium alloy increased significantly with increasing temperature. It can be seen that the rare earth phases in the alloy, i.e., the Mg-Y-Gd square phase in the WGZ1152 alloy and the Mg₂₄(Gd,Y)₅ phase in GW103K, can improve the wear resistance of the magnesium alloy and obtain better high-temperature wear resistance by improving the high-temperature mechanical properties of the alloy [140,141]. In the authors' work on the frictional wear of Mg-Gd-Y alloys, it was found that peel wear occurs at lower speeds, whereas most studies suggest that peel wear occurs at high speeds. Under reciprocal friction conditions at 200 °C, the wear rate of the alloy decreases, but the size of the chips increases. The scans show that the chips adhere to the friction surface and act as a protective layer. An et al. [142] investigated the frictional wear properties of the Mg₉₇Zn₁Y₂ alloy and compared it with the AZ91 alloy. The results show that the friction coefficient and wear rate of this alloy are lower than those of the AZ91 alloy at high loads, due to the good thermal stability and high temperature mechanical properties of the intergranular compound of the Mg₉₇Zn₁Y₂ alloy. The strengthening phase in the AZ91 alloy is the Mg₁₇Al₁₂ phase, which melts at a very low temperature and rapidly softens and coarsens when the temperature rises, losing the strengthening effect. The Mg₁₂YZn phase at the grain boundaries of the Mg₉₇Zn₁Y₂ alloy has good thermal stability, maintains a certain proportion at elevated temperatures, and continues to provide reinforcement. The role of rare earths in increasing the wear resistance of magnesium alloys mainly has two aspects: (1) Inhibit tissue loosening and reduce defects, hence reducing the

generation of crack sources during friction. (2) By adding the rare earths elements, they can form needle-like or block-like new phases with other elements, which are not easy to fall off from the matrix. Besides, new phases have higher chemical stability and higher melting points. The diffusion rate of rare earth elements is very slow when temperature rises, which can effectively hinder the sliding of grain boundaries and the propagation of cracks, thereby improving the high temperature properties of the alloy.

Itoi et al. [143] compared four materials: pure magnesium, the AZ31 alloy, the AZ91 alloy, and the $Mg_{90.5}Cu_{3.25}Y_{6.25}$ alloy (where a long period phase is present), and they found that the wear rate of the $Mg_{90.5}Cu_{3.25}Y_{6.25}$ alloy was significantly less than that of the AZ31 and AZ91 alloys at high loads. As determined by XRD and EBSD analysis, the base surfaces of both the magnesium and long period phases were parallel to the wear surface after the friction test. Magnesium substrates are susceptible to slip deformation at low critical shear stresses, so forming a substrate parallel to the friction surface has a negative impact on wear resistance. The $Mg_{90.5}Cu_{3.25}Y_{6.25}$ alloy, on the other hand, produces kink deformations in the long-period phase after friction (these kink deformations can be observed in the longitudinal section at the wear site), making parallel movement between the base and wear surfaces difficult, therefore significantly improving wear resistance. In addition, the high hardness of the long period phase is responsible for the high wear resistance of the $Mg_{90.5}Cu_{3.25}Y_{6.25}$ alloy.

4. In Vitro, In Vivo, and Clinical Experimental Studies of Magnesium Alloys

4.1. Biocompatibility Studies In Vitro

The organisation of Mg-based metals can be improved by adding alloying elements or adjusting heat treatment regimes and processing methods, thereby modulating their degradation properties and biocompatibility [144,145]. To date, magnesium alloys in various alloy systems such as Mg-Ca, Mg-Sr, Mg-Zn, Mg-Sn, Mg-Cu, and Mg-Nd-Zn-Zr have been developed, and their biocompatibility has been investigated.

4.1.1. Mg-Ca Series Alloys

Ca is an essential metal element and is involved in a large number of metabolic activities in the body. Moreover, Ca is the main inorganic component of bones and teeth and has good biocompatibility. As an alloying element for Mg, the addition of Ca not only enhances the mechanical properties of the alloy, but it also improves the corrosion resistance and biocompatibility of the alloy [146–149]. Gu et al. [150] prepared Mg-3Ca binary alloys using two smelting methods: single-roll melt spinning and casting, and they showed that the Mg-3Ca binary alloys prepared by single-roll melt spinning had better corrosion resistance and were not toxic to mouse fibroblasts (L-929) compared to the casting method, with better cell adhesion and proliferation than the casting method. Yin et al. [151] developed new Mg-Zn-Ca ternary alloys with Ca contents of 1%, 2%, and 3% (mass fraction, below) using 99.99% pure Mg ingots, 99.99% Zn pellets, and a Mg-25% Ca master alloy as raw materials, respectively. It was shown that the Mg-5Zn-1% Ca ternary alloy was not cytotoxic and did not kill red blood cells. Li et al. [152] found that the cell viability of the extracts of an extruded Mg-1Ca alloy co-cultured with L-929 cells for 2, 4, and 7 d was significantly higher than that of the control group, showing improved in vitro cytocompatibility.

4.1.2. Mg-Sr Series Alloys

Sr and Ca are homologous elements with similar chemical properties and biological functions. Sr is an essential trace element that regulates the differentiation of bone marrow mesenchymal stem cells (BMSCs) into osteoblasts and promotes the synthesis and precipitation of bone matrix proteins. Thus, Sr has a promotional effect on osteoblast differentiation and bone formation [153]. In addition, the addition of Sr can effectively improve the mechanical properties and corrosion resistance of magnesium alloys [154–156]. The study of Mg-Sr alloys has therefore attracted widespread interest from researchers.

Currently, there are more studies reported on binary Mg-Sr alloys. Tie et al. [157] conducted a biocompatibility study on water-quenched and age-treated Mg-1Sr binary alloys. After culturing primary human osteoblasts on the surface of the material, it was found that the Mg-1Sr binary alloy exhibited a higher cell survival rate than pure Mg. Comparisons of the haemolytic properties of the two Mg-based metals revealed that the haemolysis rate of Mg-1Sr was only 2.54%, which meets the minimum requirement for the haemolysis rate of medical implants (less than 5%), and the haemolysis rate of pure Mg was as high as 7.13%, indicating that the addition of Sr is beneficial for improving the cytocompatibility and haemocompatibility of Mg-based metals. Gu et al. [155] investigated the cytocompatibility of Mg-xSr binary alloys (Sr = 1–4%) in the rolled state and showed that Mg-2Sr alloys exhibited the least cytotoxicity and the highest ALP activity compared to other Sr-containing alloys, showing the best in vitro cytocompatibility. Bor-napour et al. [153] co-cultured Mg-0.5Sr alloy extract with human umbilical vein vascular endothelial cells (HUVECs) for 1, 4, and 7 d and found that cell survival was greater than 95%, indicating that the Mg-0.5Sr extract did not produce any toxic or adverse effects on HUVECs. In addition, they found that the degradation of the Mg-Sr alloy resulted in the formation of a layer of hydroxyapatite (HA) with Sr replacing Ca, which facilitated bone mineralisation and tissue healing. In addition, studies on the biocompatibility of Sr-containing multi-Mg alloys have also been reported, with Li et al. [158] finding that the degradation rate of ternary Mg-1Zn-xSr alloys increased significantly when the Sr content exceeded 0.8%. In vitro studies on Mg-1Zn-0.8Sr revealed that its extract promoted the proliferation and growth of L-929 cells, indicating that the degradation product has good cytocompatibility and that strontium alloying of Mg-Zn alloys is also expected to be used in the development of new orthopaedic implant materials. Wang et al. [159] introduced two elements, Sr and Ca, into the Mg-Si binary alloy to develop a new Mg-1.38Si-xSr-yCa quaternary alloy. In vitro studies have shown that the Mg-Si-Sr-Ca tetrameric alloy can effectively promote the proliferation of mouse pre-cranial osteogenic fine (MC3T3-E1) with a cytotoxicity grade of 0~1, meeting the biosafety criteria for orthopaedic clinical applications. Numerous studies have shown that the addition of Sr significantly contributes to the in vitro cytocompatibility, haemocompatibility, and osteogenesis of magnesium alloys.

4.1.3. Mg-Zn Series Alloys

Zn is an essential trace element and a component of biological enzymes and transcription factors. It is associated with stabilising the normal structure and function of proteins and plays an extremely important role in important physiological processes such as skeletal growth and development, reproductive genetics, immunity, and endocrinology in humans [160,161]. In addition, Zn can improve the mechanical properties of Mg through solid solution strengthening and secondary strengthening, while being able to improve the corrosion resistance of Mg [162]. In a study of binary Mg-Zn alloys, Yu et al. [163] evaluated the in vitro biocompatibility of extruded Mg-6Zn alloys. When intestinal epithelial cells (IEC-6) were co-cultured in 20% and 40% alloy extracts for 1, 3, and 5 d, reverse transcription-polymerase chain reaction (RT-PCR) assays showed that the expression levels of intestinal epithelial tight junction-related genes Occludin and ZO-1 mRNA were higher than those of the control group. It indicates that its extracts can induce the expression of tightly linked related genes at certain concentrations. Yan et al. [162] used powder metallurgy to introduce Zn into magnesium-based metals to obtain Mg-Zn binary alloys with different Zn contents. It was found that increasing the Zn content increased the micro-electro-coupling corrosion of the alloy and increased the corrosion rate. The extruded Mg-6.2% Zn can be aged to reduce the segregation of Zn, resulting in a denser and more uniform layer of corrosion products on the metal surface and improved corrosion resistance. Cytocompatibility experiments evaluating Mg-6.2% Zn binary alloys revealed that the alloy was not toxic to L-929 cells. In a study of multi-magnesium alloys containing Zn, He et al. [164] developed a Mg-1Ca-0.5Sr-xZn ($x = 0, 2, 4, \text{ and } 6$, mass fraction, %) tetrametallic alloy. In vitro studies have shown that the Mg-1Ca-0.5Sr-6Zn alloy not only

has good antibacterial properties but also effectively promotes the proliferation of MC3T3-E1 cells and exhibits good biocompatibility. The Mg-Zn series of alloys developed so far has a high potential for clinical application, as it has outstanding performance in enabling bones and fighting bacterial infections.

4.1.4. Mg-Sn Series Alloys

Sn is an important element in the body, is relatively non-toxic, has a high biosafety profile, and can be excreted via the kidneys [165]. The addition of Sn elements to Mg-based metals not only improves the strength of Mg-based metals at room temperature but also reduces the secondary dendrite spacing in the α -Mg phase, thereby refining the structure [166–168]. Zhao et al. [167] developed a Mg-Sn binary alloy using a subrapid solidification technique. It was found that, as the Sn content increased, the increase in the second phase Mg_2Sn made the corrosion resistance decrease. In vitro experiments have shown that the cytotoxicity levels of the two alloys, Mg-1Sn and Mg-3Sn, are 0 to 1, meeting the cytotoxicity requirements for orthopaedic implant materials. Next, they reported on extruded Mg-Sn binary alloys on the basis of subrapid solidification [168] and found that the extruded Mg-Sn binary alloys were similarly non-cytotoxic. The good cytocompatibility exhibited by Mg-Sn binary alloys provides a basis for their use as in vivo implant materials, but little research has been reported on their histocompatibility and haemocompatibility.

4.1.5. Mg-Cu Series Alloys

Cu is a trace element that is an important component of many enzymes in the human body. Cu also plays an important role in the immune system [169,170], restoring the rate of bone resorption to normal levels [171] and promoting the deposition of collagen fibres [172]. A lack of Cu affects osteoinduction and osteoclast activity [173], in addition to Cu's ability to stimulate endothelial cell proliferation and promote angiogenesis [174,175]. Liu et al. [176] developed a new degradable Mg-Cu binary alloy and found that the metal ions and OH⁻ dissolved by the degradation of Mg-Cu alloy did not produce cytotoxicity to HUVECs cells and MC3T3-E1 cells in a cytocompatibility study. In particular, the Mg-0.03Cu extract was effective in increasing the survival rate, ALP activity, extracellular matrix mineralisation, collagen secretion, and expression of osteogenic-related genes and proteins in MC3T3-E1 cells compared with pure Mg extract. It also promotes the expression of genes and proteins related to cell proliferation and migration, endothelial tubule formation, and angiogenesis in HUVECs. In addition, the Mg-Cu binary alloy has long-lasting antibacterial properties and is expected to be used in orthopaedic clinics in the future [177]. Although the study of Mg-Cu binary alloys is still in its infancy, their excellent biocompatibility and antibacterial properties both in vivo and ex vivo make them highly promising for future clinical applications.

4.1.6. Mg-Nd-Zn-Zr Alloys

Compared to conventional commercial alloys AZ31, WE43, and pure Mg, the new medical Mg-Nd-Zn-Zr (JDBM) quaternary alloy uses Nd, Zn, and Zr as alloying elements with high biosafety compared to the conventional commercial alloys AZ31, WE43, and pure Mg. The alloy not only has good strength and a toughness match, but it also exhibits a different corrosion degradation pattern from most magnesium alloys in a body fluid environment, i.e., homogeneous degradation, thus showing a unique advantage among many medical magnesium alloys [178,179]. Wang et al. [180,181] found that the JDBM alloy was not toxic to MC3T3-E1 cells and did not affect the normal growth of the cells. Wang et al. [182] systematically compared the effects of the JDBM alloy and pure Mg on MC3T3-E1 cells by scanning electron microscopy (SEM) observation, a cellular thiazole blue staining (MTT) assay, and a succinomyacin staining assay. The JDBM alloy was found to be effective in promoting the adhesion, proliferation, and mineralisation of MC3T3-E1 cells. By the JDBM alloy's superior corrosion resistance to pure Mg, the appropriate degradation rate as an implant material provides a suitable growth environment for cells and facilitates cytocompatibility.

Liao et al. [183] investigated the compatibility of JDBM alloys with chondrocytes for the application of magnesium-based metals in cartilage tissue engineering. The results showed no significant differences in the cytotoxicity of the JDBM alloy and in the expression of the chondrocyte-associated genes type II collagen mRNA and aggregated proteoglycan mRNA compared to pure Mg, indicating that the JDBM alloy has similar chondrocyte compatibility to pure Mg. Wang et al. [184] investigated the haemocompatibility of JDBM alloys and showed that the effects of JDBM alloys on blood cell aggregation and platelet and protein adsorption were not significantly different from Ti-6Al-4V, indicating that JDBM alloys have good haemocompatibility. JDBM alloys exhibit uniform and controlled degradation characteristics, good ex vivo cytocompatibility, histocompatibility, and haemocompatibility, giving them potential for clinical application. Table 2 [150–153,155,158,159,162,167,176,180,185] summarises the effects of alloying on the cytocompatibility of biomedical Mg-based metals. Overall, most of the new biomedical magnesium-based metals developed through alloying exhibit good cytocompatibility and haemocompatibility and have good application prospects.

Table 2. In vitro cellular biocompatibility of different magnesium alloys.

Alloy	Processing	Test Cells	Cell Viability Assay	Cell Culture Time (Day)							References	
				One	Two	Three	Four	Five	Six	Seven		
Mg-3Ca	Rapid solidified	L-929	MTT	>90	>90		>90					[150]
Mg-5Zn-1Ca	As-cast	L-929	MTT		>100		>90				>80	[151]
Mg-1Ca	As-extruded	L-929	MTT		>90		>90				>90	[152]
Mg-0.5Sr	As-cast	HUVECs	Alamar blue	>95			>100				>110	[153]
Mg-1Sr	As-cast	MG63	MTT	>70		>90		>80				[155]
pure Mg	As-rolled	MG63	MTT	>60		>70		>70				[155]
Mg-1Zn-0.8Sr	Backward extruded	L-929	MTT	>80	>90	>100						[158]
Mg-1.38Si-0.5Sr-0.6Ca	As-cast	MC3T3-E1	CCK-8	>60		>100		>100				[159]
Mg-6%Zn	As-extruded	L-929	MTT	>80			>80				>80	[162]
Mg-Zn	As-cast	rBMSCs	CCK-8	>50		>70		>90				[185]
Mg-1Sn	Sub-rapid solidified	MG63	MTT		>100		>100			>100		[167]
Mg-3Sn	Sub-rapid solidified	MG63	MTT		>100		>100			>100		[167]
Mg-0.03Cu	As-cast	MC3T3-E1	MTT	>100		>100		>100				[176]
		HUVECs		>100		>100		>100				
Mg-Nd-Zn-Zr		MC3T3-E1	MTT	>70			>90				>80	[180]

4.2. In Vivo Biocompatibility Studies

The element Al is an element commonly used to improve the properties of magnesium alloys. Yu et al. [186] established a rabbit femoral defect model to evaluate the degradation and bone volume changes in fluorine-coated magnesium–aluminium alloy porous scaffolds and found that the fluorine coating enhanced the corrosion resistance of the magnesium alloy and made it more biocompatible, inducing more new bone formation. Miura et al. [187] implanted magnesium–aluminium alloy plates into the head, dorsal subcutaneous, and femoral subperiosteum of rats and found that they corroded fastest in the head, followed by the dorsal, and they were the slowest in the femur. There was also vascularised fibrous capsule formation around the plate that matured over time, and the loss of alloy volume at different anatomical sites was found to correlate with capsule thickness. A study by Sato et al. [188] also found that magnesium alloy plates showed the fastest volume reduction in the abdomen, followed by the head, back, tibia, and femur. The fluorine-coated magnesium–aluminium alloy in the above study showed good biocompatibility, and the rate of degradation in the animals was found to be related to their environment, which could be a guide for future clinical work.

As another essential trace element in the human body, Zn is involved in various physiological reactions and has good biocompatibility. Jiang et al. [189] investigated the biodegradation properties and biological characteristics of MgF₂-coated magnesium alloys, implanted with MgF₂-coated and uncoated magnesium alloys into rabbit femurs. The results showed a more uniform increase in the density of the surrounding cancellous bone and the relative structural integrity of the bone trabeculae in the coated group. This leads to the conclusion that the MgF₂ coating is effective in reducing the *in vivo* degradation rate of magnesium alloys, delaying the release of magnesium ions, and that the coating itself has good biocompatibility and bioactivity. Zhang et al. [190] conducted a similar study and found that micro-arc oxidised Mg-Zn-Ca alloy scaffolds were effective in repairing critical bone defects. It also improves the bone repair effect, corrosion resistance, and biocompatibility of the Mg-Zn-Ca alloy scaffold. The results of these studies confirm that the surface coating of magnesium alloys can effectively improve the corrosion resistance of magnesium alloys, resulting in better biocompatibility and bone repair. Li et al. [191] constructed magnesium-based implants integrated with the anti-catabolic drug zoledronic acid. The results of 12 weeks of implantation of intramedullary nail fixation of femoral fractures in a rat model of osteoporosis showed that the magnesium-based implant enhanced the repair of osteoporotic fractures by promoting bone crust formation compared to conventional stainless steel, and that the treatment in combination with the implant-coated topical release of zoledronic acid further improved bone regeneration rates. Significant improvements were observed in bone quality and mechanical strength due to the synergistic effect of the two, which inhibits osteoclasts and bone remodelling. *In vitro* and *in vivo* studies have shown that it stimulates new bone formation while inhibiting bone remodelling, which is attributed to the local release of magnesium degradation products and zoledronic acid. This suggests that magnesium-based implants can slowly release magnesium-based degradation products and zoledronic acid in a controlled manner and can be a superior alternative for osteoporosis-related fracture reconstruction. This experiment confirms that the magnesium-based implant enhances fracture repair in animals with osteoporotic fractures, suggesting that this biodegradable magnesium alloy orthopaedic implant has great potential and may, in the future, replace the internal fixation devices currently used to treat osteoporotic fractures. Such studies combining magnesium alloys with specific drugs where the two work synergistically could inform the design of clinical trials. Xu et al. [192] studied the performance of magnesium–zinc alloy scaffolds in anterior cervical discectomy and fusion in sheep and assessed the surface degradation of magnesium–zinc alloy scaffolds modified by micro-arc oxidation. The results show that the scaffold had ideal biocompatibility and biomechanical properties, but the fusion status, as assessed radiologically and histologically, was poor. The degradation rate of the Mg-Zn alloy scaffold was controlled but slower than expected by micro-arc oxidation modification, ultimately showing that the scaffold degraded in an over-controlled and fusion-failed manner. This shows that further research is needed in the future to improve the properties of this type of magnesium-based material and to provide an experimental basis for future clinical applications. Ca is one of the most alloying elements of magnesium, and its addition not only enhances the mechanical properties of the alloy, but it also improves the corrosion resistance of the alloy. Some researchers found that, after 4 weeks of the implantation of the magnesium–calcium alloy into rat femurs, the alloy implant was well-integrated with the surrounding bone, and slow and uniform degradation could be observed without adverse effects on the surrounding tissue, suggesting that the alloy could be used as a new temporary implant material [193].

In addition, in order to improve the mechanical properties and corrosion resistance of the alloy, rare earth elements are also used as an effective element to improve the properties of the alloy. Schaller et al. [194] conducted a study of WE43 in a porcine rib model, where a coated WE43 plate/screw system, an uncoated WE43 plate/screw system, and a titanium plate/screw system were implanted into porcine ribs; the main components were yttrium (Y), zirconium (Zr), and rare earth metals (RE), where W represents the element yttrium,

E represents the element rare earth, 4 represents the mass percentage of yttrium, and 3 represents the mass percentage of rare earth elements. The results revealed a higher amount of gas formation in the group of uncoated magnesium plates fixed to the ribs. A total of 12 weeks after surgery, there was better bone healing around the coated group compared to the uncoated group, and no negative effects of magnesium degradation on bone healing were observed upon histological examination. This study shows that WE43 with coatings has good osteogenic properties and provides positive support for the further development of magnesium plate/screw systems for bone fixation. Lin et al. [195] constructed functionalised $\text{TiO}_2/\text{Mg}_2\text{TiO}_4$ nanospheres on the surface of WE43 using a plasma immersion ion implantation technique and performed animal studies. A study showing a significant increase in new bone formation around ionomer-infiltrated treated magnesium compared to controls at 12 weeks post-operation, with the Young's modulus of the new bone being 82% of that of the surrounding mature bone. In addition, this particular $\text{TiO}_2/\text{Mg}_2\text{TiO}_4$ layer was found to exhibit some bacterial disinfection when irradiated by UV light, which was attributed to the production of intracellular reactive oxygen species. From these observations, it can be concluded that $\text{TiO}_2/\text{Mg}_2\text{TiO}_4$ nanolayers on magnesium implants treated by ionomer immersion can significantly promote new bone formation and inhibit bacterial infection while improving the corrosion resistance of magnesium alloys. Marukawa et al. [196] assessed the biological response of the WE43 implant in vivo and its effectiveness as a plate/screw fixation system. The WE43 magnesium alloy and poly-L-lactic acid are materials commonly used in clinical practice to assess the effectiveness of magnesium implants as a plate/screw fixation system using a canine tibial fracture model. WE43 was found to be strong enough to fix and support the healing of canine tibial fractures. This study shows its great potential for use in orthopaedics, oral and maxillofacial surgery, etc., for fracture fixation in load-bearing areas, so these biodegradable magnesium alloys can be considered good candidates to replace biodegradable polymers. Oshibe et al. [197] studied the degradation and biocompatibility of WE43 by implanting WE43 round rods with and without anodic oxidation into rat tibiae. At 1 year post-operation, mature bone structures appeared around the implants in both groups, indicating that the WE43 implants show good long-term stability and biocompatibility in the bone tissue. Torroni et al. [198] tested the biocompatibility and degradation properties of untreated (cast) and artificially aged (T5) WE43 as subperiosteal implants on a sheep model. Studies have shown that both alloys exhibit excellent biocompatibility, with WE43-as (as-cast) showing a higher degradation rate and increased bone remodelling capacity. WE43-T5 shows greater stability at the bone/implant interface and is more suitable for manufacturing intraperiosteal screws. In this investigator's previous study, WE43-as and WE43-T5 were implanted subperiosteally in the frontal nasal region of sheep to test local biocompatibility. The results showed that the WE43-T5 alloy had stronger mechanical properties compared to WE43-as, and both alloys showed good biocompatibility and osteogenesis-promoting properties [199]. The scholar's study confirms the excellent biocompatibility and bone-enabling ability of WE43, providing the basis for further research into the use of magnesium alloys in the maxillofacial fracture environment, and it demonstrates that WE43-T5 exhibits higher stability and lower degradation rates than WE43-as. Niu et al. [200] used JDBM screws coated with DCPD (mainly $\text{CaHPO}_4 \cdot 2\text{H}_2\text{O}$) to implant in rabbit mandibles. A total of 7 months after implantation, the screws had been largely degraded, and the screw necks were fractured and largely unsupported. After 18 months of implantation, the screw had lost its original shape, and the remaining volume was only about 10.7% of the original volume, as shown in Figure 12. Bai et al. [201] prepared composite coatings on magnesium alloy surfaces using the micro-arc oxidation technique and coated the coatings for 2 h and 24 h using hydrothermal deposition. The results of implanting each of the prepared samples into rabbit femoral marrow cavities showed that the degradation rate of the composite-coated magnesium alloy was slowed down and that the degradation rate of the composite-coated magnesium alloy after a 24 h hydrothermal treatment was slower than that of the magnesium alloy after a 2 h hydrothermal treatment. The study shows

that hydrothermal deposition can further slow down the degradation of magnesium alloys based on the micro-arc oxidation technique, which provides a basis for future research directions. The results of the animal experiments with magnesium alloy implants are shown in Table 3.

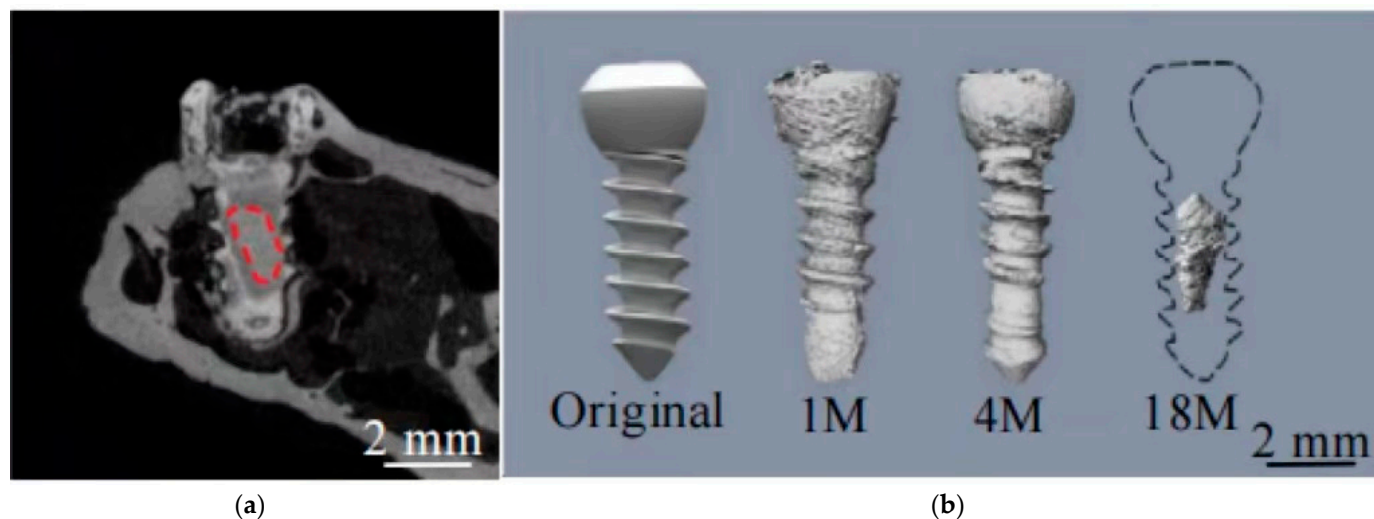


Figure 12. CT scans and 3D reconstruction of JDBM screw after 18 months implantation: (a) CT image of implanted screw (the original screw is marked by a red dashed line); (b) the original screw and segmented residual screw at 1, 4, and 18 months post-operation [200]. Reprinted with permission from [200]. 2016, Elsevier.

Table 3. Results of in vivo tests on the biocompatibility of magnesium alloy implants.

Alloy Types and Author	Implant Form and Site	Duration of Implantation (Weeks)	Degradation	References
Magnesium and aluminium alloy Miura et al.	Metal plates; rat ventral, head, dorsum, and femur	4	Abdomen > Head > Back > Femur Bone	[187]
Magnesium and aluminium alloy Sato et al.	Metal plates; rat ventral, head, back, tibia, femur	4	Abdomen > Head, Back > Tibia Bone and femur	[188]
Magnesium and aluminium alloy Yu et al.	Porous scaffold, rabbit femur	18	Reduce	[186]
Magnesium-zinc-zirconium alloy Jiang et al.	Screws, rabbit femur	24	Reduce	[189]
Magnesium-zinc-zirconium alloy Li et al.	Intramedullary nail, rat femur	12	Reduce	[191]
Magnesium, zinc and calcium alloys Zhang et al.	Stents, rabbit ulna	12	Reduce	[190]

Table 3. Cont.

Alloy Types and Author	Implant Form and Site	Duration of Implantation (Weeks)	Degradation	References
Magnesium rare earth alloys Bai et al.	Intramedullary nail, rabbit femoral medullary cavity	12	Reduce	[201]
Magnesium rare earth alloys Torrioni et al.	Plate nail fixation system, sheep forehead, nasal bone	6	Reduce	[199]
Magnesium rare earth alloys Marukawa et al.	Bone screws, canine tibia	4	Not described	[196]
Magnesium rare earth alloys Oshibe et al.	Intramedullary nail, rat tibia	48	Volume loss after 48 weeks 27.7%	[197]
Magnesium rare earth alloys Lin et al.	Screws, rat femur	12	Reduce	[195]
Calcium magnesium alloy Cihova et al.	Intramedullary nail, rat femur	4	Reduce	[193]

4.3. Clinical Trial Studies

Even though no study has yet clarified which alloy has the best therapeutic effect (Table 4), a number of in vivo animal studies have confirmed the good therapeutic effect of different magnesium alloys. As a new type of orthopaedic implant, magnesium alloys have achieved certain clinical progress, where Mg-Y-RE-Zr (magnesium–yttrium–rare earth element–zirconium) alloys, Mg-5Ca-1Zn alloys, and also pure magnesium have all been clinically tested. In 2010, Plaass used Mg-Y-RE-Zr screws from Syntellix, Germany, for bunion orthopaedic surgery, and the fracture ends healed well after surgery without adverse effects in patients [202]. The company subsequently introduced magnesium screws for the treatment of extremity fractures and non-union fractures, all with good results [66,68]. In 2013, in a clinical trial for the treatment of bunions, Syntellix, Germany, observed the radiographs of the distal metatarsal foot of one 29-year-old woman (Figure 13). The screw almost completely remodelled the bone 16 months after surgery. This clinical trial obtained the CE mark on the biodegradable magnesium alloy screw [66]. In 2015, Mg-Ca-Zn screws manufactured in Korea were approved for clinical use in the treatment of non-healing internal fixation of navicular and distal radius fractures, with clinical observations showing that patients had good fracture line healing and that the screws could be completely degraded within 6~18 months [68]. Pure magnesium screws were used for free iliac bone grafting in femoral head necrosis by Zhao Dewei, Zhongshan Hospital, Dalian University. At a 1-year post-operative follow-up, bone growth around the degraded screws was significantly better than in the control group, showing good osteogenic properties [69]. These clinical trials all used single pure magnesium or a magnesium alloy screw, implanted in a non-weight bearing area, with good clinical results. It is still unknown whether the magnesium alloy endoskeleton is able to provide sufficient mechanical strength, considering that, in the future, it may be used in long bones that need to provide strong support or torsional forces. Hel-mecke et al. used Mg-Y-RE-Zr magnesium alloy interference screws to fix artificial ligaments to artificial bone, which required more force to extract than ordinary interference screws and provided better stability for ligament fixation [203]. None of the current clinical trials have had significant gas accumulation in the bone and soft tissues surrounding pure magnesium and magnesium alloy screws. Only radiolucent areas are seen in the surrounding bone as well as a small amount of gas accumulation in the surrounding soft tissues, with the former disappearing within 4–6 weeks post-operation and the gas in the soft tissues being completely absorbed within 2 months post-operation [66,68]. The reason for the small amount of gas may be related to the relatively small size of the screw in relation to the body. If a larger number of screws or larger magnesium plates or prostheses are used at a later stage, the degradation process may produce a large amount of gas that collects

in the surrounding tissue. Control of the rate of degradation is particularly important at this time, and slowing down the rate of degradation is key to controlling gas production. Current clinical trials have demonstrated that pure magnesium and magnesium alloy screws provide the required support at the site for orthopaedic clinical applications, while being highly biocompatible and not degrading too rapidly [66,68]. The clinical trials have provided valuable data and a solid foundation for future clinical applications of magnesium alloys in orthopaedics. As more clinical trials are conducted, they will be a huge boost for the use of magnesium alloys in orthopaedics.

Table 4. Clinical trials with magnesium alloys.

Magnesium Alloy Material Types	Part	Sample Numbers	Country	Degree of Healing	References
Mg-Y-RE-Zr screws	Bunion correction	13	Germany	All healed	[202]
Mg-5 wt%Ca-1 wt%Zn	Internal fixation of fractures of the metacarpal and carpal bones	53	Korea	All healed	[68]
Mg-Y-RE-Zr screws	Bunion orthopaedics	40	Germany	79% healing after 6 weeks, 90% healing after 12 weeks	[202]
Pure magnesium screws	Femoral head ischaemic necrosis graft tape; vascular bone flap fixation	48	China	No displacement or collapse of bone flap after operation	[69]
Mg-Y-RE-Zr screws	Bunion orthopaedics	100	Germany	All healed	[202]



(a)



(b)

Figure 13. Cont.

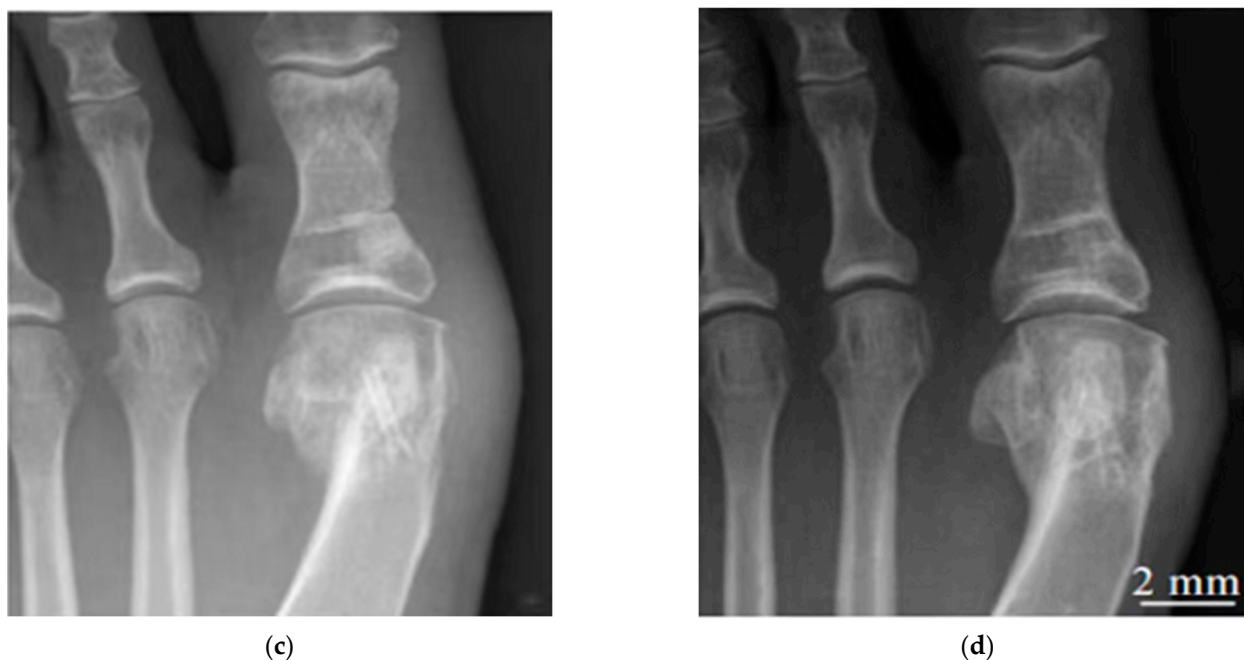


Figure 13. Before operation (a), 6 weeks after operation (b), 12 weeks after operation (c), and 16 months after operation (d) [66].

5. Conclusions and Outlook

Despite significant developments and numerous achievements in the field of medical magnesium alloys for bone repair in recent years, a number of fundamental scientific questions remain to be further elucidated. (1) Mechanisms of in vivo degradation of magnesium alloys: Various factors in the complex environment of the human body, such as different cells, the composition of body fluids, force conditions, etc., can affect the degradation behaviour of magnesium alloys, and only by examining the influence of these factors can the degradation of magnesium implants in the human body be finally predicted, and the design of magnesium implants can be further guided. (2) The metabolic pathways of the absorption of magnesium alloys in the body, with particular reference to the metabolic mechanisms of the alloying elements: This relates to the biosafety basis of magnesium alloys and is a question that must be answered before clinical application. In addition, although our research scholars have achieved world-recognised first-class results in the field of biodegradable medical magnesium alloys, they have lagged behind Germany and South Korea in terms of clinical application and transformation, and there is an urgent need to accelerate the domestic magnesium alloy clinical transformation process. This requires the cooperation of researchers, government review experts, and companies. It is believed that, in the near future, our self-developed biodegradable medical magnesium alloy will be able to be widely promoted clinically for the benefit of patients.

Author Contributions: Writing—original draft preparation, P.Z., L.L. and Z.L.; investigation and visualisation, J.C. and Q.Z.; supervision, J.Z. and Y.F.; funding acquisition, C.L., Z.L. and Y.F. All authors have read and agreed to the published version of the manuscript.

Funding: This research was funded by Versus Arthritis UK (Grant No: 21977); the European Commission via a H2020-MSCA-RISE programme (BAMOS, Grant No: 734156); Innovative UK via Newton Fund (Grant No: 102872); and the Engineering and Physical Science Research Council (EPSRC) via DTP CASE programme (Grant No: EP/T517793/1).

Institutional Review Board Statement: Not applicable.

Informed Consent Statement: Not applicable.

Conflicts of Interest: The authors declare no conflict of interest.

References

1. Kalfas, I.H. Principles of Bone Healing. *Neurosurg. Focus* **2001**, *10*, 1–4. [[CrossRef](#)] [[PubMed](#)]
2. Nuss, K.M.R.; von Rechenberg, B. Biocompatibility Issues with Modern Implants in Bone—A Review for Clinical Orthopedics. *Open Orthop. J.* **2008**, *2*, 66–78. [[CrossRef](#)] [[PubMed](#)]
3. Westerman, R.W.; Scammell, B.E. Principles of Bone and Joint Injuries and Their Healing. *Surgery* **2012**, *30*, 54–60. [[CrossRef](#)]
4. Liu, C.; Wan, P.; Tan, L.L.; Wang, K.; Yang, K. Preclinical Investigation of an Innovative Magnesium-Based Bone Graft Substitute for Potential Orthopaedic Applications. *J. Orthop. Transl.* **2014**, *2*, 139–148. [[CrossRef](#)]
5. Lee, J.Y.; Han, G.; Kim, Y.C.; Byun, J.Y.; Jang, J.I.; Seok, H.K.; Yang, S.J. Effects of Impurities on the Biodegradation Behavior of Pure Magnesium. *Met. Mater. Int.* **2009**, *15*, 955–961. [[CrossRef](#)]
6. Tan, L.; Yu, X.; Wan, P.; Yang, K. Biodegradable Materials for Bone Repairs: A Review. *J. Mater. Sci. Technol.* **2013**, *29*, 503–513. [[CrossRef](#)]
7. Stark, J.G. Use of Selective Estrogen Receptor Modulator for Joint Fusion and Other Repair or Healing of Connective Tissue. Available online: <https://www.freepatentsonline.com/8933028.html> (accessed on 7 November 2013).
8. Calori, G.M.; Mazza, E.; Colombo, M.; Ripamonti, C. The Use of Bone-Graft Substitutes in Large Bone Defects: Any Specific Needs? *Injury* **2011**, *42*, S56–S63. [[CrossRef](#)]
9. Van der Stok, J.; van Lieshout, E.M.M.; El-Massoudi, Y.; van Kralingen, G.H.; Patka, P. Bone Substitutes in the Netherlands—A Systematic Literature Review. *Acta Biomater.* **2011**, *7*, 739–750. [[CrossRef](#)]
10. Auer, J.A.; von Rechenberg, B.; Bohner, M.; Hofmann-Antenbrink, M. *Bone Grafts and Bone Replacements*; Elsevier: Amsterdam, The Netherlands, 2012; pp. 1081–1095. [[CrossRef](#)]
11. Kim, H.M. Ceramic Bioactivity and Related Biomimetic Strategy. *Curr. Opin. Solid State Mater. Sci.* **2003**, *7*, 289–299. [[CrossRef](#)]
12. Dias, A.G.; Lopes, M.A.; Gibson, I.R.; Santos, J.D. In Vitro Degradation Studies of Calcium Phosphate Glass Ceramics Prepared by Controlled Crystallization. *J. Non-Cryst. Solids* **2003**, *330*, 81–89. [[CrossRef](#)]
13. Aoki, S.; Yamaguchi, S.; Nakahira, A.; Suganuma, K. A New Approach to an Artificial Joint Based on Bio-Cartilage/Porous β -Tricalcium Phosphate System. *J. Eur. Ceram. Soc.* **2003**, *23*, 2939–2946. [[CrossRef](#)]
14. Mohamed, K.R.; Beherei, H.H.; El-Rashidy, Z.M. In Vitro Study of Nano-Hydroxyapatite/Chitosan–Gelatin Composites for Bio-Applications. *J. Adv. Res.* **2014**, *5*, 201–208. [[CrossRef](#)] [[PubMed](#)]
15. Yoganand, C.P.; Selvarajan, V.; Cannillo, V.; Sola, A.; Roumeli, E.; Goudouri, O.M.; Paraskevopoulos, K.M.; Rouabhia, M. Characterization and in Vitro-Bioactivity of Natural Hydroxyapatite Based Bio-Glass–Ceramics Synthesized by Thermal Plasma Processing. *Ceram. Int.* **2010**, *36*, 1757–1766. [[CrossRef](#)]
16. Giannoudis, P.V.; Dinopoulos, H.; Tsiridis, E. Bone Substitutes: An Update. *Injury* **2005**, *36*, S20–S27. [[CrossRef](#)]
17. Böstman, O.; Pihlajamäki, H. Clinical Biocompatibility of Biodegradable Orthopaedic Implants for Internal Fixation: A Review. *Biomaterials* **2000**, *21*, 2615–2621. [[CrossRef](#)]
18. Chai, H.; Guo, L.; Wang, X.; Fu, Y.; Guan, J.; Tan, L.; Ren, L.; Yang, K. Antibacterial Effect of 317L Stainless Steel Contained Copper in Prevention of Implant-Related Infection in Vitro and in Vivo. *J. Mater. Sci. Mater. Med.* **2011**, *22*, 2525–2535. [[CrossRef](#)]
19. Nan, L.; Yang, K. Cu Ions Dissolution from Cu-Bearing Antibacterial Stainless Steel. *J. Mater. Sci. Technol.* **2010**, *26*, 941–944. [[CrossRef](#)]
20. Shirai, T.; Tsuchiya, H.; Shimizu, T.; Ohtani, K.; Zen, Y.; Tomita, K. Prevention of Pin Tract Infection with Titanium–Copper Alloys. *J. Biomed. Mater. Res. B Appl. Biomater.* **2009**, *91B*, 373–380. [[CrossRef](#)]
21. Nakai, M.; Niinomi, M.; Ishii, D. Mechanical and Biodegradable Properties of Porous Titanium Filled with Poly-L-Lactic Acid by Modified in Situ Polymerization Technique. *J. Mech. Behav. Biomed. Mater.* **2011**, *4*, 1206–1218. [[CrossRef](#)]
22. Staiger, M.P.; Pietak, A.M.; Huadmai, J.; Dias, G. Magnesium and Its Alloys as Orthopedic Biomaterials: A Review. *Biomaterials* **2006**, *27*, 1728–1734. [[CrossRef](#)]
23. Erdmann, N.; Angrisani, N.; Reifenrath, J.; Lucas, A.; Thorey, F.; Bormann, D.; Meyer-Lindenberg, A. Biomechanical Testing and Degradation Analysis of MgCa0.8 Alloy Screws: A Comparative in Vivo Study in Rabbits. *Acta Biomater.* **2011**, *7*, 1421–1428. [[CrossRef](#)] [[PubMed](#)]
24. Tschernitschek, H.; Borchers, L.; Geurtsen, W. Nonalloyed Titanium as a Bioinert Metal—A Review. *J. Prosthet. Dent.* **2006**, *96*, 12. [[CrossRef](#)]
25. Hong, D.; Saha, P.; Chou, D.T.; Lee, B.; Collins, B.E.; Tan, Z.; Dong, Z.; Kumta, P.N. In Vitro Degradation and Cytotoxicity Response of Mg–4% Zn–0.5% Zr (ZK40) Alloy as a Potential Biodegradable Material. *Acta Biomater.* **2013**, *9*, 8534–8547. [[CrossRef](#)] [[PubMed](#)]
26. Yeung, K.W.K.; Wong, K.H.M. Biodegradable Metallic Materials for Orthopaedic Implantations: A Review. *Technol. Health Care* **2012**, *20*, 345–362. [[CrossRef](#)]
27. Shadanbaz, S.; Dias, G.J. Calcium Phosphate Coatings on Magnesium Alloys for Biomedical Applications: A Review. *Acta Biomater.* **2012**, *8*, 20–30. [[CrossRef](#)]
28. Yang, H.; Yan, X.; Ling, M.; Xiong, Z.; Ou, C.; Lu, W. In Vitro Corrosion and Cytocompatibility Properties of Nano-Whisker Hydroxyapatite Coating on Magnesium Alloy for Bone Tissue Engineering Applications. *Int. J. Mol. Sci.* **2015**, *16*, 6113–6123. [[CrossRef](#)]
29. Lin, X.; Tan, L.; Zhang, Q.; Yang, K.; Hu, Z.; Qiu, J.; Cai, Y. The in Vitro Degradation Process and Biocompatibility of a ZK60 Magnesium Alloy with a Forsterite-Containing Micro-Arc Oxidation Coating. *Acta Biomater.* **2013**, *9*, 8631–8642. [[CrossRef](#)]

30. Persaud-Sharma, D.; Mcgoron, A. Biodegradable Magnesium Alloys: A Review of Material Development and Applications. *J. Biomim. Biomater. Tissue Eng.* **2011**, *12*, 25–39. [[CrossRef](#)]
31. Musso, C.G. Magnesium Metabolism in Health and Disease. *Int. Urol. Nephrol.* **2009**, *41*, 357–362. [[CrossRef](#)]
32. Vormann, J. Magnesium: Nutrition and Metabolism. *Mol. Asp. Med.* **2003**, *24*, 27–37. [[CrossRef](#)]
33. Zhang, Y.; Xu, J.; Ruan, Y.C.; Yu, M.K.; O’Laughlin, M.; Wise, H.; Chen, D.; Tian, L.; Shi, D.; Wang, J.; et al. Implant-Derived Magnesium Induces Local Neuronal Production of CGRP to Improve Bone-Fracture Healing in Rats. *Nat. Med.* **2016**, *22*, 1160–1169. [[CrossRef](#)]
34. Waizy, H.; Seitz, J.M.; Reifenrath, J.; Weizbauer, A.; Bach, F.W.; Meyer-Lindenberg, A.; Denkena, B.; Windhagen, H. Biodegradable Magnesium Implants for Orthopedic Applications. *J. Mater. Sci.* **2012**, *48*, 39–50. [[CrossRef](#)]
35. Bornapour, M.; Celikin, M.; Cerruti, M.; Pekguleryuz, M. Magnesium Implant Alloy with Low Levels of Strontium and Calcium: The Third Element Effect and Phase Selection Improve Bio-Corrosion Resistance and Mechanical Performance. *Mater. Sci. Eng. C* **2014**, *35*, 267–282. [[CrossRef](#)] [[PubMed](#)]
36. Xue, D.; Yun, Y.; Schulz, M.J.; Shanov, V. Corrosion Protection of Biodegradable Magnesium Implants Using Anodization. *Mater. Sci. Eng. C* **2011**, *31*, 215–223. [[CrossRef](#)]
37. Seal, C.K.; Vince, K.; Hodgson, M.A. Biodegradable Surgical Implants Based on Magnesium Alloys—A Review of Current Research. *IOP Conf. Ser. Mater. Sci. Eng.* **2009**, *4*, 012011. [[CrossRef](#)]
38. Brar, H.S.; Wong, J.; Manuel, M.V. Investigation of the Mechanical and Degradation Properties of Mg–Sr and Mg–Zn–Sr Alloys for Use as Potential Biodegradable Implant Materials. *J. Mech. Behav. Biomed. Mater.* **2012**, *7*, 87–95. [[CrossRef](#)] [[PubMed](#)]
39. Li, N.; Zheng, Y. Novel Magnesium Alloys Developed for Biomedical Application: A Review. *J. Mater. Sci. Technol.* **2013**, *29*, 489–502. [[CrossRef](#)]
40. Chen, Y.; Xu, Z.; Smith, C.; Sankar, J. Recent Advances on the Development of Magnesium Alloys for Biodegradable Implants. *Acta Biomater.* **2014**, *10*, 4561–4573. [[CrossRef](#)]
41. Yun, Y.H.; Dong, Z.; Yang, D.; Schulz, M.J.; Shanov, V.N.; Yarmolenko, S.; Xu, Z.; Kumta, P.; Sfeir, C. Biodegradable Mg Corrosion and Osteoblast Cell Culture Studies. *Mater. Sci. Eng. C* **2009**, *29*, 1814–1821. [[CrossRef](#)]
42. Song, G.; Song, S. A Possible Biodegradable Magnesium Implant Material. *Adv. Eng. Mater.* **2007**, *9*, 298–302. [[CrossRef](#)]
43. Agarwal, S.; Curtin, J.; Duffy, B.; Jaiswal, S. Biodegradable Magnesium Alloys for Orthopaedic Applications: A Review on Corrosion, Biocompatibility and Surface Modifications. *Mater. Sci. Eng. C* **2016**, *68*, 948–963. [[CrossRef](#)] [[PubMed](#)]
44. Gu, X.N.; Zheng, W.; Cheng, Y.; Zheng, Y.F. A Study on Alkaline Heat Treated Mg–Ca Alloy for the Control of the Biocorrosion Rate. *Acta Biomater.* **2009**, *5*, 2790–2799. [[CrossRef](#)]
45. Lloyd, A.W. Interfacial Bioengineering to Enhance Surface Biocompatibility. *Med. Device Technol.* **2002**, *13*, 18–21. [[PubMed](#)]
46. Jebson, P.J.L.; Hayden, R.J. AO Principles of Fracture Management. *JAMA* **2008**, *300*, 2432–2433. [[CrossRef](#)]
47. Kuhlmann, J.; Bartsch, I.; Willbold, E.; Schuchardt, S.; Holz, O.; Hort, N.; Höche, D.; Heineman, W.R.; Witte, F. Fast Escape of Hydrogen from Gas Cavities around Corroding Magnesium Implants. *Acta Biomater.* **2013**, *9*, 8714–8721. [[CrossRef](#)] [[PubMed](#)]
48. Wang, H.; Shi, Z. In Vitro Biodegradation Behavior of Magnesium and Magnesium Alloy. *J. Biomed. Mater. Res. B Appl. Biomater.* **2011**, *98B*, 203–209. [[CrossRef](#)]
49. Witte, F.; Hort, N.; Vogt, C.; Cohen, S.; Kainer, K.U.; Willumeit, R.; Feyerabend, F. Degradable Biomaterials Based on Magnesium Corrosion. *Curr. Opin. Solid State Mater. Sci.* **2008**, *12*, 63–72. [[CrossRef](#)]
50. Gill, P.; Munroe, N.; Dua, R.; Ramaswamy, S. Corrosion and Biocompatibility Assessment of Magnesium Alloys. *J. Biomater. Nanobiotechnol.* **2012**, *3*, 10–13. [[CrossRef](#)]
51. Hornberger, H.; Virtanen, S.; Boccaccini, A.R. Biomedical Coatings on Magnesium Alloys—A Review. *Acta Biomater.* **2012**, *8*, 2442–2455. [[CrossRef](#)]
52. Chen, J.; Tan, L.; Yang, K. Recent Advances on the Development of Biodegradable Magnesium Alloys: A Review. *Mater. Technol.* **2016**, *31*, 681–688. [[CrossRef](#)]
53. Paramsothy, M.; Ramakrishna, S. Biodegradable Materials for Clinical Applications: A Review. *Rev. Adv. Sci. Eng.* **2016**, *4*, 221–238. [[CrossRef](#)]
54. Pogorielov, M.; Husak, E.; Solodivnik, A.; Zhdanov, S. Magnesium-Based Biodegradable Alloys: Degradation, Application, and Alloying Elements. *Interv. Med. Appl. Sci.* **2017**, *9*, 27. [[CrossRef](#)] [[PubMed](#)]
55. Payr, E. Beiträge zur Technik der Blutgefäß- und Nervennaht Nebst Mittheilungen Über Die Verwendung Eines Resorbirbaren Metalles in Der Chirurgie. *Arch. Klin. Chir.* **1900**, *62*, 67–93.
56. Lambotte, A. Technique et Indications de La Prothèse Perdue Dans Le Traitement des Fractures. *Press Med Belge.* **1909**, *17*, 321–323.
57. Verbrugge, J. Le Matériel Métallique Résorbable En Chirurgie Osseuse. *Presse Med.* **1934**, *23*, 460–465.
58. McBride, E.D. Absorbable metal in bone surgery: A further report on the use of magnesium alloys. *J. Am. Med. Assoc.* **1938**, *111*, 2464–2467. [[CrossRef](#)]
59. Maier, O. Über Die Verwendbarkeit von Leichtmetallen in Der Chirurgie (Metallisches Magnesium Als Reizmittel Zur Knochenneubildung). *Dtsch. Z. Chir.* **1940**, *253*, 552–556. [[CrossRef](#)]
60. Troitskii, V.V.; Tsitrin, D.N. The Resorbing Metallic Alloy “Osteosinthezit” as Material for Fastening Broken Bone. *Khirurgiia.* **1944**, *8*, 41–44.
61. Witte, F. The History of Biodegradable Magnesium Implants: A Review. *Acta Biomater.* **2010**, *6*, 1680–1692. [[CrossRef](#)]

62. Witte, F.; Kaese, V.; Haferkamp, H.; Switzer, E.; Meyer-Lindenberg, A.; Wirth, C.J.; Windhagen, H. In Vivo Corrosion of Four Magnesium Alloys and the Associated Bone Response. *Biomaterials* **2005**, *26*, 3557–3563. [[CrossRef](#)]
63. Witte, F.; Ulrich, H.; Palm, C.; Willbold, E. Biodegradable Magnesium Scaffolds: Part II: Peri-Implant Bone Remodeling. *J. Biomed. Mater. Res. A* **2007**, *81A*, 757–765. [[CrossRef](#)] [[PubMed](#)]
64. Staiger, M.P.; Kolbeinsson, I.; Kirkland, N.T.; Nguyen, T.; Dias, G.; Woodfield, T.B.F. Synthesis of Topologically-Ordered Open-Cell Porous Magnesium. *Mater. Lett.* **2010**, *64*, 2572–2574. [[CrossRef](#)]
65. Windhagen, H.; Radtke, K.; Weizbauer, A.; Diekmann, J.; Noll, Y.; Kreimeyer, U.; Schavan, R.; Stukenborg-Colsman, C.; Waizy, H. Biodegradable Magnesium-Based Screw Clinically Equivalent to Titanium Screw in Hallux Valgus Surgery: Short Term Results of the First Prospective, Randomized, Controlled Clinical Pilot Study. *Biomed. Eng. Online* **2013**, *12*, 62. [[CrossRef](#)] [[PubMed](#)]
66. Plaass, C.; Ettinger, S.; Sonnow, L.; Koenneker, S.; Noll, Y.; Weizbauer, A.; Reifenrath, J.; Claassen, L.; Daniilidis, K.; Stukenborg-Colsman, C.; et al. Early Results Using a Biodegradable Magnesium Screw for Modified Chevron Osteotomies. *J. Orthop. Res.* **2016**, *34*, 2207–2214. [[CrossRef](#)]
67. Seitz, J.M.; Lucas, A.; Kirschner, M. Magnesium-Based Compression Screws: A Novelty in the Clinical Use of Implants. *JOM* **2016**, *68*, 1177–1182. [[CrossRef](#)]
68. Lee, J.W.; Han, H.S.; Han, K.J.; Park, J.; Jeon, H.; Ok, M.R.; Seok, H.K.; Ahn, J.P.; Lee, K.E.; Lee, D.H.; et al. Long-Term Clinical Study and Multiscale Analysis of in Vivo Biodegradation Mechanism of Mg Alloy. *Proc. Natl. Acad. Sci. USA* **2016**, *113*, 716–721. [[CrossRef](#)]
69. Zhao, D.; Huang, S.; Lu, F.; Wang, B.; Yang, L.; Qin, L.; Yang, K.; Li, Y.; Li, W.; Wang, W.; et al. Vascularized Bone Grafting Fixed by Biodegradable Magnesium Screw for Treating Osteonecrosis of the Femoral Head. *Biomaterials* **2016**, *81*, 84–92. [[CrossRef](#)]
70. Danish, M.; Ginta, T.L.; Habib, K.; Carou, D.; Rani, A.M.A.; Saha, B.B. Thermal Analysis during Turning of AZ31 Magnesium Alloy under Dry and Cryogenic Conditions. *Int. J. Adv. Manuf. Technol.* **2017**, *91*, 2855–2868. [[CrossRef](#)]
71. Carou, D.; Rubio, E.M.; Davim, J.P. Analysis of Ignition Risk in Intermittent Turning of UNS M11917 Magnesium Alloy at Low Cutting Speeds Based on the Chip Morphology. *Proc. Inst. Mech. Eng. Part B J. Eng. Manuf.* **2014**, *229*, 365–371. [[CrossRef](#)]
72. Bertolini, R.; Bruschi, S.; Ghiotti, A.; Pezzato, L.; Dabalà, M. The Effect of Cooling Strategies and Machining Feed Rate on the Corrosion Behavior and Wettability of AZ31 Alloy for Biomedical Applications. *Procedia CIRP* **2017**, *65*, 7–12. [[CrossRef](#)]
73. Davis, R.; Singh, A. Performance Study of Cryo-Treated End Mill Via Wet, Cryogenic, and Hybrid Lubri-Coolant-Milling Induced Surface Integrity of Biocompatible Mg Alloy AZ91D. *Proc. Inst. Mech. Eng. C J. Mech. Eng. Sci* **2021**, *235*, 7045–7061. [[CrossRef](#)]
74. Davis, R.; Singh, A. Tailoring Surface Integrity of Biomedical Mg Alloy AZ31B Using Distinct End Mill Treatment Conditions and Machining Environments. *J. Mater. Eng. Perform.* **2020**, *29*, 7617–7635. [[CrossRef](#)]
75. Wen, P.; Qin, Y.; Chen, Y.; Voshage, M.; Jauer, L.; Poprawe, R.; Schleifenbaum, J.H. Laser Additive Manufacturing of Zn Porous Scaffolds: Shielding Gas Flow, Surface Quality and Densification. *J. Mater. Sci. Technol.* **2019**, *35*, 368–376. [[CrossRef](#)]
76. Al-Kazzaz, H.; Medraj, M.; Cao, X.; Jahazi, M. Nd:YAG Laser Welding of Aerospace Grade ZE41A Magnesium Alloy: Modeling and Experimental Investigations. *Mater. Chem. Phys.* **2008**, *109*, 61–76. [[CrossRef](#)]
77. Wei, K.; Gao, M.; Wang, Z.; Zeng, X. Effect of Energy Input on Formability, Microstructure and Mechanical Properties of Selective Laser Melted AZ91D Magnesium Alloy. *Mater. Sci. Eng. A* **2014**, *611*, 212–222. [[CrossRef](#)]
78. Zhang, Z.; Kong, F.; Kovacevic, R. Laser Hot-Wire Cladding of Co-Cr-W Metal Cored Wire. *Opt. Lasers Eng.* **2020**, *128*, 105998. [[CrossRef](#)]
79. Li, N.; Huang, S.; Zhang, G.; Qin, R.; Liu, W.; Xiong, H.; Shi, G.; Blackburn, J. Progress in Additive Manufacturing on New Materials: A Review. *J. Mater. Sci. Technol.* **2019**, *35*, 242–269. [[CrossRef](#)]
80. Wang, Y.; Chen, X.; Kononov, S.V. Additive Manufacturing Based on Welding Arc: A Low-Cost Method. *J. Surf. Investig. X-ray Synchrotron Neutron Tech.* **2018**, *11*, 1317–1328. [[CrossRef](#)]
81. Li, J.L.Z.; Alkahari, M.R.; Rosli, N.A.B.; Hasan, R.; Sudin, M.N.; Ramli, F.R. Review of Wire Arc Additive Manufacturing for 3d Metal Printing. *Int. J. Autom. Technol.* **2019**, *13*, 346–353. [[CrossRef](#)]
82. Wu, B.; Pan, Z.; Ding, D.; Cuiuri, D.; Li, H.; Xu, J.; Norrish, J. A Review of the Wire Arc Additive Manufacturing of Metals: Properties, Defects and Quality Improvement. *J. Manuf. Process.* **2018**, *35*, 127–139. [[CrossRef](#)]
83. Takagi, H.; Sasahara, H.; Abe, T.; Sannomiya, H.; Nishiyama, S.; Ohta, S.; Nakamura, K. Material-Property Evaluation of Magnesium Alloys Fabricated Using Wire-and-Arc-Based Additive Manufacturing. *Addit. Manuf.* **2018**, *24*, 498–507. [[CrossRef](#)]
84. Unocic, R.R.; DuPont, J.N. Process Efficiency Measurements in the Laser Engineered Net Shaping Process. *Metall. Mater. Trans. B* **2004**, *35*, 143–152. [[CrossRef](#)]
85. Pierron, N.; Sallamand, P.; Mattei, S. Study of Magnesium and Aluminum Alloys Absorption Coefficient during Nd:YAG Laser Interaction. *Appl. Surf. Sci.* **2007**, *253*, 3208–3214. [[CrossRef](#)]
86. Ding, D.; Pan, Z.; Cuiuri, D.; Li, H. Wire-Feed Additive Manufacturing of Metal Components: Technologies, Developments and Future Interests. *Int. J. Adv. Manuf. Technol.* **2015**, *81*, 465–481. [[CrossRef](#)]
87. Braszczyńska-Malik, K.N.; Mróz, M. Gas-Tungsten Arc Welding of AZ91 Magnesium Alloy. *J. Alloys Compd.* **2011**, *509*, 9951–9958. [[CrossRef](#)]
88. Ng, C.C.; Savalani, M.M.; Man, H.C.; Gibson, I. Layer Manufacturing of Magnesium and Its Alloy Structures for Future Applications. *Virtual Phys. Prototyp.* **2010**, *5*, 13–19. [[CrossRef](#)]
89. Shen, X.; Ma, G.; Chen, P. Effect of Welding Process Parameters on Hybrid GMAW-GTAW Welding Process of AZ31B Magnesium Alloy. *Int. J. Adv. Manuf. Technol.* **2017**, *94*, 2811–2819. [[CrossRef](#)]

90. Chiu, K.Y.; Wong, M.H.; Cheng, F.T.; Man, H.C. Characterization and Corrosion Studies of Fluoride Conversion Coating on Degradable Mg Implants. *Surf. Coat. Technol.* **2007**, *202*, 590–598. [[CrossRef](#)]
91. Witte, F.; Fischer, J.; Nellesen, J.; Vogt, C.; Vogt, J.; Donath, T.; Beckmann, F. In Vivo Corrosion and Corrosion Protection of Magnesium Alloy LAE442. *Acta Biomater.* **2010**, *6*, 1792–1799. [[CrossRef](#)]
92. Seitz, J.M.; Collier, K.; Wulf, E.; Bormann, D.; Bach, F.W. Comparison of the Corrosion Behavior of Coated and Uncoated Magnesium Alloys in an In Vitro Corrosion Environment. *Adv. Eng. Mater.* **2011**, *13*, B313–B323. [[CrossRef](#)]
93. Maurya, R.; Siddiqui, A.R.; Balani, K. An Environment-Friendly Phosphate Chemical Conversion Coating on Novel Mg-9Li-7Al-1Sn and Mg-9Li-5Al-3Sn-1Zn Alloys with Remarkable Corrosion Protection. *Appl. Surf. Sci.* **2018**, *443*, 429–440. [[CrossRef](#)]
94. Sankara Narayanan, T.S.N.; Park, I.S.; Lee, M.H. Strategies to Improve the Corrosion Resistance of Microarc Oxidation (MAO) Coated Magnesium Alloys for Degradable Implants: Prospects and Challenges. *Prog. Mater. Sci.* **2014**, *60*, 1–71. [[CrossRef](#)]
95. Gu, X.N.; Li, N.; Zhou, W.R.; Zheng, Y.F.; Zhao, X.; Cai, Q.Z.; Ruan, L. Corrosion Resistance and Surface Biocompatibility of a Microarc Oxidation Coating on a Mg–Ca Alloy. *Acta Biomater.* **2011**, *7*, 1880–1889. [[CrossRef](#)] [[PubMed](#)]
96. Gao, J.H.; Guan, S.K.; Chen, J.; Wang, L.G.; Zhu, S.J.; Hu, J.H.; Ren, Z.W. Fabrication and Characterization of Rod-like Nano-Hydroxyapatite on MAO Coating Supported on Mg–Zn–Ca Alloy. *Appl. Surf. Sci.* **2011**, *257*, 2231–2237. [[CrossRef](#)]
97. Cui, L.Y.; Zeng, R.C.; Guan, S.K.; Qi, W.C.; Zhang, F.; Li, S.Q.; Han, E.H. Degradation Mechanism of Micro-Arc Oxidation Coatings on Biodegradable Mg–Ca Alloys: The Influence of Porosity. *J. Alloys Compd.* **2017**, *695*, 2464–2476. [[CrossRef](#)]
98. Wang, H.X.; Guan, S.K.; Wang, X.; Ren, C.X.; Wang, L.G. In Vitro Degradation and Mechanical Integrity of Mg–Zn–Ca Alloy Coated with Ca-Deficient Hydroxyapatite by the Pulse Electrodeposition Process. *Acta Biomater.* **2010**, *6*, 1743–1748. [[CrossRef](#)]
99. Song, Y.; Zhang, S.; Li, J.; Zhao, C.; Zhang, X. Electrodeposition of Ca–P Coatings on Biodegradable Mg Alloy: In Vitro Biomineralization Behavior. *Acta Biomater.* **2010**, *6*, 1736–1742. [[CrossRef](#)]
100. Keim, S.; Brunner, J.G.; Fabry, B.; Virtanen, S. Control of Magnesium Corrosion and Biocompatibility with Biomimetic Coatings. *J. Biomed. Mater. Res. B Appl Biomater.* **2011**, *96B*, 84–90. [[CrossRef](#)]
101. Zhang, Y.; Zhang, G.; Wei, M. Controlling the Biodegradation Rate of Magnesium Using Biomimetic Apatite Coating. *J. Biomed. Mater. Res. B Appl Biomater.* **2009**, *89B*, 408–414. [[CrossRef](#)] [[PubMed](#)]
102. Gray-Munro, J.E.; Strong, M. The Mechanism of Deposition of Calcium Phosphate Coatings from Solution onto Magnesium Alloy AZ31. *J. Biomed. Mater. Res. A* **2009**, *90A*, 339–350. [[CrossRef](#)]
103. Wang, Q.; Tan, L.; Xu, W.; Zhang, B.; Yang, K. Dynamic Behaviors of a Ca–P Coated AZ31B Magnesium Alloy during in Vitro and in Vivo Degradations. *Mater. Sci. Eng. B* **2011**, *176*, 1718–1726. [[CrossRef](#)]
104. Hu, J.; Zhang, C.; Cui, B.; Bai, K.; Guan, S.; Wang, L.; Zhu, S. In Vitro Degradation of AZ31 Magnesium Alloy Coated with Nano TiO₂ Film by Sol–Gel Method. *Appl. Surf. Sci.* **2011**, *257*, 8772–8777. [[CrossRef](#)]
105. Roy, A.; Singh, S.S.; Datta, M.K.; Lee, B.; Ohodnicki, J.; Kumta, P.N. Novel Sol–Gel Derived Calcium Phosphate Coatings on Mg4Y Alloy. *Mater. Sci. Eng. B* **2011**, *176*, 1679–1689. [[CrossRef](#)]
106. Wan, Y.Z.; Xiong, G.Y.; Luo, H.L.; He, F.; Huang, Y.; Wang, Y.L. Influence of Zinc Ion Implantation on Surface Nanomechanical Performance and Corrosion Resistance of Biomedical Magnesium–Calcium Alloys. *Appl. Surf. Sci.* **2008**, *254*, 5514–5516. [[CrossRef](#)]
107. Wu, G.S.; Zeng, X.Q.; Yao, S.S.; Han, H.B. Ion Implanted AZ31 Magnesium Alloy. *Mater. Sci. Forum* **2007**, *546–549*, 551–554. [[CrossRef](#)]
108. Li, J.N.; Cao, P.; Zhang, X.N.; Zhang, S.X.; He, Y.H. In Vitro Degradation and Cell Attachment of a PLGA Coated Biodegradable Mg–6Zn Based Alloy. *J. Mater. Sci.* **2010**, *45*, 6038–6045. [[CrossRef](#)]
109. Wong, H.M.; Yeung, K.W.K.; Lam, K.O.; Tam, V.; Chu, P.K.; Luk, K.D.K.; Cheung, K.M.C. A Biodegradable Polymer-Based Coating to Control the Performance of Magnesium Alloy Orthopaedic Implants. *Biomaterials* **2010**, *31*, 2084–2096. [[CrossRef](#)] [[PubMed](#)]
110. Wang, Y.; Tie, D.; Guan, R.; Wang, N.; Shang, Y.; Cui, T.; Li, J. Microstructures, Mechanical Properties, and Degradation Behaviors of Heat-Treated Mg–Sr Alloys as Potential Biodegradable Implant Materials. *J. Mech. Behav. Biomed. Mater.* **2017**, *77*, 47–57. [[CrossRef](#)]
111. Ibrahim, H.; Klarner, A.D.; Poorganji, B.; Dean, D.; Luo, A.A.; Elahinia, M. Microstructural, Mechanical and Corrosion Characteristics of Heat-Treated Mg-1.2Zn-0.5Ca (Wt%) Alloy for Use as Resorbable Bone Fixation Material. *J. Mech. Behav. Biomed. Mater.* **2017**, *69*, 203–212. [[CrossRef](#)]
112. Maier, P.; Peters, R.; Mendis, C.L.; Müller, S.; Hort, N. Influence of Precipitation Hardening in Mg–Y–Nd on Mechanical and Corrosion Properties. *JOM* **2015**, *68*, 1183–1190. [[CrossRef](#)]
113. Tan, L.; Dong, J.; Chen, J.; Yang, K. Development of Magnesium Alloys for Biomedical Applications: Structure, Process to Property Relationship. *Mater. Technol.* **2017**, *33*, 235–243. [[CrossRef](#)]
114. el Mahallawy, N.; Ahmed Diaa, A.; Akdesir, M.; Palkowski, H. Effect of Zn Addition on the Microstructure and Mechanical Properties of Cast, Rolled and Extruded Mg-6Sn-XZn Alloys. *Mater. Sci. Eng. A* **2017**, *680*, 47–53. [[CrossRef](#)]
115. Li, K.; Injeti, V.S.Y.; Trivedi, P.; Murr, L.E.; Misra, R.D.K. Nanoscale Deformation of Multiaxially Forged Ultrafine-Grained Mg-2Zn-2Gd Alloy with High Strength-High Ductility Combination and Comparison with the Coarse-Grained Counterpart. *J. Mater. Sci. Technol.* **2018**, *34*, 311–316. [[CrossRef](#)]
116. Krajčák, T.; Minárik, P.; Stráská, J.; Gubicza, J.; Máthis, K.; Janeček, M. Influence of the Initial State on the Microstructure and Mechanical Properties of AX41 Alloy Processed by ECAP. *J. Mater. Sci.* **2018**, *54*, 3469–3484. [[CrossRef](#)]

117. Habibnejad-Korayem, M.; Mahmudi, R.; Ghasemi, H.M.; Poole, W.J. Tribological Behavior of Pure Mg and AZ31 Magnesium Alloy Strengthened by Al₂O₃ Nano-Particles. *Wear* **2010**, *268*, 405–412. [[CrossRef](#)]
118. Das, S.; Morales, A.T.; Alpas, A.T. Microstructural Evolution during High Temperature Sliding Wear of Mg–3% Al–1% Zn (AZ31) Alloy. *Wear* **2010**, *268*, 94–103. [[CrossRef](#)]
119. Zafari, A.; Ghasemi, H.M.; Mahmudi, R. Effect of Rare Earth Elements Addition on the Tribological Behavior of AZ91D Magnesium Alloy at Elevated Temperatures. *Wear* **2013**, *303*, 98–108. [[CrossRef](#)]
120. Asl, K.M.; Tari, A.; Khomamizadeh, F. Effect of Deep Cryogenic Treatment on Microstructure, Creep and Wear Behaviors of AZ91 Magnesium Alloy. *Mater. Sci. Eng. A* **2009**, *523*, 27–31. [[CrossRef](#)]
121. Chen, H.; Alpas, A.T. Sliding Wear Map for the Magnesium Alloy Mg–9Al–0.9 Zn (AZ91). *Wear* **2000**, *246*, 106–116. [[CrossRef](#)]
122. Wang, S.Q.; Yang, Z.R.; Zhao, Y.T.; Wei, M.X. Sliding Wear Characteristics of AZ91D Alloy at Ambient Temperatures of 25–200 °C. *Tribol. Lett.* **2010**, *38*, 39–45. [[CrossRef](#)]
123. Huang, W.J.; Lin, Q.; Liu, C.L. Tribological Behaviour of AZ71E Alloy at High Temperatures. *Trans. Nonferrous Met. Soc. China* **2012**, *22*, 2057–2065. [[CrossRef](#)]
124. Aung, N.N.; Zhou, W.; Lim, L.E.N. Wear Behaviour of AZ91D Alloy at Low Sliding Speeds. *Wear* **2008**, *265*, 780–786. [[CrossRef](#)]
125. El-Morsy, A.W. Dry Sliding Wear Behavior of Hot Deformed Magnesium AZ61 Alloy as Influenced by the Sliding Conditions. *Mater. Sci. Eng. A* **2008**, *473*, 330–335. [[CrossRef](#)]
126. Zafari, A.; Ghasemi, H.M.; Mahmudi, R. Tribological Behavior of AZ91D Magnesium Alloy at Elevated Temperatures. *Wear* **2012**, *292–293*, 33–40. [[CrossRef](#)]
127. Yang, Z.R.; Wei, M.X.; Zhao, Y.T.; Wang, S.Q. Dry Sliding Wear Behavior and Mechanism of AM60B Alloy at 25–200 °C. *Trans. Nonferrous Met. Soc. China* **2011**, *21*, 2584–2591. [[CrossRef](#)]
128. Guo, W.; Wang, Q.; Ye, B.; Zhou, H. Enhanced Microstructure Homogeneity and Mechanical Properties of AZ31–Si Composite by Cyclic Closed-Die Forging. *J. Alloys Compd.* **2013**, *552*, 409–417. [[CrossRef](#)]
129. Ajith Kumar, K.K.; Pillai, U.T.S.; Pai, B.C.; Chakraborty, M. Dry Sliding Wear Behaviour of Mg–Si Alloys. *Wear* **2013**, *303*, 56–64. [[CrossRef](#)]
130. Mehta, D.S.; Masood, S.H.; Song, W.Q. Investigation of Wear Properties of Magnesium and Aluminum Alloys for Automotive Applications. *J. Mater. Process. Technol.* **2004**, *155–156*, 1526–1531. [[CrossRef](#)]
131. Hu, B.; Peng, L.; Yang, Y.; Ding, W. Effect of Solidification Conditions on Microstructure, Mechanical and Wear Properties of Mg–5Al–3Ca–0.12Sr Magnesium Alloy. *Mater. Des.* **2010**, *31*, 3901–3907. [[CrossRef](#)]
132. Matsuoka, T.; Sakaguchi, K.; Mukai, T.; Matsuyama, M.; Yoshioka, R. Effects of the Grain Size on Friction and Wear Properties of ZK60 Magnesium Alloy. *Zair. J. Soc. Mater. Sci. Jpn.* **2002**, *51*, 1154–1159. [[CrossRef](#)]
133. Meshinchi Asl, K.; Masoudi, A.; Khomamizadeh, F. The Effect of Different Rare Earth Elements Content on Microstructure, Mechanical and Wear Behavior of Mg–Al–Zn Alloy. *Mater. Sci. Eng. A* **2010**, *527*, 2027–2035. [[CrossRef](#)]
134. Somekawa, H.; Maeda, S.; Hirayama, T.; Matsuoka, T.; Inoue, T.; Mukai, T. Microstructural Evolution during Dry Wear Test in Magnesium and Mg–Y Alloy. *Mater. Sci. Eng. A* **2013**, *561*, 371–377. [[CrossRef](#)]
135. Liu, Y.; Shao, S.; Xu, C.; Yang, X.; Lu, D. Enhancing Wear Resistance of Mg–Zn–Gd Alloy by Cryogenic Treatment. *Mater. Lett.* **2012**, *76*, 201–204. [[CrossRef](#)]
136. Selvan, S.A.; Ramanathan, S. Dry Sliding Wear Behavior of As-Cast ZE41A Magnesium Alloy. *Mater. Des.* **2010**, *31*, 1930–1936. [[CrossRef](#)]
137. López, A.J.; Rodrigo, P.; Torres, B.; Rams, J. Dry Sliding Wear Behaviour of ZE41A Magnesium Alloy. *Wear* **2011**, *271*, 2836–2844. [[CrossRef](#)]
138. Hu, M.L.; Wang, Q.D.; Li, C.; Ding, W.J. Dry Sliding Wear Behavior of Cast Mg–11Y–5Gd–2Zn Magnesium Alloy. *Trans. Nonferrous Met. Soc. China* **2012**, *22*, 1918–1923. [[CrossRef](#)]
139. Hu, M.; Wang, Q.; Chen, C.; Yin, D.; Ding, W.; Ji, Z. Dry Sliding Wear Behaviour of Mg–10Gd–3Y–0.4Zr Alloy. *Mater. Des.* **2012**, *42*, 223–229. [[CrossRef](#)]
140. He, S.M.; Zeng, X.Q.; Peng, L.M.; Gao, X.; Nie, J.F.; Ding, W.J. Precipitation in a Mg–10Gd–3Y–0.4Zr (Wt.%) Alloy during Isothermal Ageing at 250 °C. *J. Alloys Compd.* **2006**, *421*, 309–313. [[CrossRef](#)]
141. Yin, D.D.; Wang, Q.D.; Gao, Y.; Chen, C.J.; Zheng, J. Effects of Heat Treatments on Microstructure and Mechanical Properties of Mg–11Y–5Gd–2Zn–0.5Zr (Wt.%) Alloy. *J. Alloys Compd.* **2011**, *509*, 1696–1704. [[CrossRef](#)]
142. An, J.; Li, R.G.; Lu, Y.; Chen, C.M.; Xu, Y.; Chen, X.; Wang, L.M. Dry Sliding Wear Behavior of Magnesium Alloys. *Wear* **2008**, *265*, 97–104. [[CrossRef](#)]
143. Itoi, T.; Gonda, K.; Hirohashi, M. Relationship of Wear Properties to Basal-Plane Texture of Worn Surface of Mg Alloys. *Wear* **2011**, *270*, 606–612. [[CrossRef](#)]
144. Ding, Y.; Wen, C.; Hodgson, P.; Li, Y. Effects of Alloying Elements on the Corrosion Behavior and Biocompatibility of Biodegradable Magnesium Alloys: A Review. *J. Mater. Chem. B* **2014**, *2*, 1912–1933. [[CrossRef](#)] [[PubMed](#)]
145. Li, X.; Liu, X.; Wu, S.; Yeung, K.W.K.; Zheng, Y.; Chu, P.K. Design of Magnesium Alloys with Controllable Degradation for Biomedical Implants: From Bulk to Surface. *Acta Biomater.* **2016**, *45*, 2–30. [[CrossRef](#)] [[PubMed](#)]
146. Kim, W.C.; Kim, J.G.; Lee, J.Y.; Seok, H.K. Influence of Ca on the Corrosion Properties of Magnesium for Biomaterials. *Mater. Lett.* **2008**, *62*, 4146–4148. [[CrossRef](#)]

147. Wan, Y.; Xiong, G.; Luo, H.; He, F.; Huang, Y.; Zhou, X. Preparation and Characterization of a New Biomedical Magnesium–Calcium Alloy. *Mater. Des.* **2008**, *29*, 2034–2037. [[CrossRef](#)]
148. Rad, H.R.B.; Idris, M.H.; Kadir, M.R.A.; Farahany, S. Microstructure Analysis and Corrosion Behavior of Biodegradable Mg–Ca Implant Alloys. *Mater. Des.* **2012**, *33*, 88–97. [[CrossRef](#)]
149. Li, Y.; Hodgson, P.D.; Wen, C. The Effects of Calcium and Yttrium Additions on the Microstructure, Mechanical Properties and Biocompatibility of Biodegradable Magnesium Alloys. *J. Mater. Sci.* **2010**, *46*, 365–371. [[CrossRef](#)]
150. Gu, X.N.; Li, X.L.; Zhou, W.R.; Cheng, Y.; Zheng, Y.F. Microstructure, Biocorrosion and Cytotoxicity Evaluations of Rapid Solidified Mg–3Ca Alloy Ribbons as a Biodegradable Material. *Biomed. Mater.* **2010**, *5*, 35013. [[CrossRef](#)]
151. Yin, P.; Li, N.F.; Lei, T.; Liu, L.; Ouyang, C. Effects of Ca on Microstructure, Mechanical and Corrosion Properties and Biocompatibility of Mg–Zn–Ca Alloys. *J. Mater. Sci. Mater. Med.* **2013**, *24*, 1365–1373. [[CrossRef](#)]
152. Li, Z.; Gu, X.; Lou, S.; Zheng, Y. The development of binary Mg–Ca alloys for use as biodegradable materials within bone. *Biomater. Guildford.* **2008**, *29*, 1329–1344. [[CrossRef](#)]
153. Bornapour, M.; Muja, N.; Shum-Tim, D.; Cerruti, M.; Pekguleryuz, M. Biocompatibility and Biodegradability of Mg–Sr Alloys: The Formation of Sr-Substituted Hydroxyapatite. *Acta Biomater.* **2013**, *9*, 5319–5330. [[CrossRef](#)] [[PubMed](#)]
154. Fan, Y.; Wu, G.H.; Zhai, C.Q. Effect of Strontium on Mechanical Properties and Corrosion Resistance of AZ91D. *Mater. Sci. Forum* **2007**, *546–549*, 567–570. [[CrossRef](#)]
155. Gu, X.N.; Xie, X.H.; Li, N.; Zheng, Y.F.; Qin, L. In Vitro and in Vivo Studies on a Mg–Sr Binary Alloy System Developed as a New Kind of Biodegradable Metal. *Acta Biomater.* **2012**, *8*, 2360–2374. [[CrossRef](#)] [[PubMed](#)]
156. Guan, R.G.; Cipriano, A.F.; Zhao, Z.Y.; Lock, J.; Tie, D.; Zhao, T.; Cui, T.; Liu, H. Development and Evaluation of a Magnesium–Zinc–Strontium Alloy for Biomedical Applications—Alloy Processing, Microstructure, Mechanical Properties, and Biodegradation. *Mater. Sci. Eng. C* **2013**, *33*, 3661–3669. [[CrossRef](#)]
157. Tie, D.; Guan, R.; Liu, H.; Cipriano, A.; Liu, Y.; Wang, Q.; Huang, Y.; Hort, N. An in Vivo Study on the Metabolism and Osteogenic Activity of Bioabsorbable Mg–1Sr Alloy. *Acta Biomater.* **2016**, *29*, 455–467. [[CrossRef](#)]
158. Li, H.; Peng, Q.; Li, X.; Li, K.; Han, Z.; Fang, D. Microstructures, Mechanical and Cytocompatibility of Degradable Mg–Zn Based Orthopedic Biomaterials. *Mater. Des.* **2014**, *58*, 43–51. [[CrossRef](#)]
159. Wang, W.; Han, J.; Yang, X.; Li, M.; Wan, P.; Tan, L.; Zhang, Y.; Yang, K. Novel Biocompatible Magnesium Alloys Design with Nutrient Alloying Elements Si, Ca and Sr: Structure and Properties Characterization. *Mater. Sci. Eng. B* **2016**, *214*, 26–36. [[CrossRef](#)]
160. Wang, C.; Lin, K.; Chang, J.; Sun, J. Osteogenesis and Angiogenesis Induced by Porous β -CaSiO₃/PDLGA Composite Scaffold via Activation of AMPK/ERK1/2 and PI3K/Akt Pathways. *Biomaterials* **2013**, *34*, 64–77. [[CrossRef](#)]
161. Jin, G.; Qin, H.; Cao, H.; Qian, S.; Zhao, Y.; Peng, X.; Zhang, X.; Liu, X.; Chu, P.K. Synergistic Effects of Dual Zn/Ag Ion Implantation in Osteogenic Activity and Antibacterial Ability of Titanium. *Biomaterials* **2014**, *35*, 7699–7713. [[CrossRef](#)]
162. Yan, Y.; Cao, H.; Kang, Y.; Yu, K.; Xiao, T.; Luo, J.; Deng, Y.; Fang, H.; Xiong, H.; Dai, Y. Effects of Zn Concentration and Heat Treatment on the Microstructure, Mechanical Properties and Corrosion Behavior of as-Extruded Mg–Zn Alloys Produced by Powder Metallurgy. *J. Alloys Compd.* **2017**, *693*, 1277–1289. [[CrossRef](#)]
163. Yu, S.; Wang, X.H.; Chen, Y.G.; Zheng, Q.; Zhang, X.N.; Zhao, C.L.; Zhang, S.X.; Yan, J. In Vitro and in Vivo Evaluation of Effects of Mg–6Zn Alloy on Tight Junction of Intestinal Epithelial Cell. *Trans. Nonferrous Met. Soc. China* **2015**, *25*, 3760–3766. [[CrossRef](#)]
164. He, G.; Wu, Y.; Zhang, Y.; Zhu, Y.; Liu, Y.; Li, N.; Li, M.; Zheng, G.; He, B.; Yin, Q.; et al. Addition of Zn to the Ternary Mg–Ca–Sr Alloys Significantly Improves Their Antibacterial Properties. *J. Mater. Chem. B* **2015**, *3*, 6676–6689. [[CrossRef](#)] [[PubMed](#)]
165. Chen, C.J.; Chen, C.W.; Wu, M.M.; Kuo, T.L. Cancer Potential in Liver, Lung, Bladder and Kidney Due to Ingested Inorganic Arsenic in Drinking Water. *Br. J. Cancer* **1992**, *66*, 888–892. [[CrossRef](#)] [[PubMed](#)]
166. Hou, L.; Li, Z.; Zhao, H.; Pan, Y.; Pavlinich, S.; Liu, X.; Li, X.; Zheng, Y.; Li, L. Microstructure, Mechanical Properties, Corrosion Behavior and Biocompatibility of As-Extruded Biodegradable Mg–3Sn–1Zn–0.5Mn Alloy. *J. Mater. Sci. Technol.* **2016**, *32*, 874–882. [[CrossRef](#)]
167. Zhao, C.; Pan, F.; Zhao, S.; Pan, H.; Song, K.; Tang, A. Microstructure, Corrosion Behavior and Cytotoxicity of Biodegradable Mg–Sn Implant Alloys Prepared by Sub-Rapid Solidification. *Mater. Sci. Eng. C* **2015**, *54*, 245–251. [[CrossRef](#)]
168. Zhao, C.; Pan, F.; Zhao, S.; Pan, H.; Song, K.; Tang, A. Preparation and Characterization of As-Extruded Mg–Sn Alloys for Orthopedic Applications. *Mater. Des.* **2015**, *70*, 60–67. [[CrossRef](#)]
169. Harris, E.D. A Requirement for Copper in Angiogenesis. *Nutr. Rev.* **2004**, *62*, 60–64. [[CrossRef](#)]
170. Harris, E. Basic and Clinical Aspects of Copper. *Crit. Rev. Clin. Lab. Sci.* **2003**, *40*, 547–586. [[CrossRef](#)]
171. Wilson, T.; Katz, J.M.; Gray, D.H. Inhibition of Active Bone Resorption by Copper. *Calcif. Tissue Int.* **1981**, *33*, 35–39. [[CrossRef](#)]
172. Gérard, C.; Bordeleau, L.J.; Barralet, J.; Doillon, C.J. The Stimulation of Angiogenesis and Collagen Deposition by Copper. *Biomaterials* **2010**, *31*, 824–831. [[CrossRef](#)]
173. Strause, L.; Saltman, P.; Glowacki, J. The Effect of Deficiencies of Manganese and Copper on Osteoinduction and on Resorption of Bone Particles in Rats. *Calcif. Tissue Int.* **1987**, *41*, 145–150. [[CrossRef](#)]
174. Sen, C.K.; Khanna, S.; Venojarvi, M.; Trikha, P.; Christopher Ellison, E.; Hunt, T.K.; Roy, S. Copper-Induced Vascular Endothelial Growth Factor Expression and Wound Healing. *Am. J. Physiol. Heart Circ. Physiol.* **2002**, *282*, H1821–H1827. [[CrossRef](#)] [[PubMed](#)]
175. Hu, D.F. Copper Stimulates Proliferation of Human Endothelial Cells under Culture. *J. Cell. Biochem.* **1998**, *69*, 326–335. [[CrossRef](#)]

176. Liu, C.; Fu, X.; Pan, H.; Wan, P.; Wang, L.; Tan, L.; Wang, K.; Zhao, Y.; Yang, K.; Chu, P.K. Biodegradable Mg-Cu Alloys with Enhanced Osteogenesis, Angiogenesis, and Long-Lasting Antibacterial Effects. *Sci. Rep.* **2016**, *6*, 27374. [[CrossRef](#)] [[PubMed](#)]
177. Li, Y.; Liu, L.; Wan, P.; Zhai, Z.; Mao, Z.; Ouyang, Z.; Yu, D.; Sun, Q.; Tan, L.; Ren, L.; et al. Biodegradable Mg-Cu Alloy Implants with Antibacterial Activity for the Treatment of Osteomyelitis: In Vitro and in Vivo Evaluations. *Biomaterials* **2016**, *106*, 250–263. [[CrossRef](#)] [[PubMed](#)]
178. Zhang, X.; Yuan, G.; Mao, L.; Niu, J.; Ding, W. Biocorrosion Properties of As-Extruded Mg–Nd–Zn–Zr Alloy Compared with Commercial AZ31 and WE43 Alloys. *Mater. Lett.* **2012**, *66*, 209–211. [[CrossRef](#)]
179. Zong, Y.; Yuan, G.; Zhang, X.; Mao, L.; Niu, J.; Ding, W. Comparison of Biodegradable Behaviors of AZ31 and Mg–Nd–Zn–Zr Alloys in Hank’s Physiological Solution. *Mater. Sci. Eng. B* **2012**, *177*, 395–401. [[CrossRef](#)]
180. Wang, Y.P.; He, Y.H.; Zhu, Z.J.; Jiang, Y.; Zhang, J.; Niu, J.L.; Mao, L.; Yuan, G.Y. In Vitro Degradation and Biocompatibility of Mg–Nd–Zn–Zr Alloy. *Chin. Sci. Bull.* **2012**, *57*, 2163–2170. [[CrossRef](#)]
181. Wang, Y.; Zhu, Z.; He, Y.; Jiang, Y.; Zhang, J.; Niu, J.; Mao, L.; Yuan, G. In Vivo Degradation Behavior and Biocompatibility of Mg–Nd–Zn–Zr Alloy at Early Stage. *Int. J. Mol. Med.* **2012**, *29*, 178–184. [[CrossRef](#)]
182. Wang, Y.; Ouyang, Y.; Peng, X.; Mao, L.; Yuan, G.; Jiang, Y.; He, Y. Effects of Degradable MG–ND–ZN–ZR Alloy on Osteoblastic Cell Function. *Int. J. Immunopathol. Pharmacol.* **2012**, *25*, 597–606. [[CrossRef](#)]
183. Liao, Y.; Ouyang, Y.; Niu, J.; Zhang, J.; Wang, Y.; Zhu, Z.; Yuan, G.; He, Y.; Jiang, Y. In Vitro Response of Chondrocytes to a Biodegradable Mg–Nd–Zn–Zr Alloy. *Mater. Lett.* **2012**, *83*, 206–208. [[CrossRef](#)]
184. Wang, Y.P.; Ouyang, Y.M.; He, Y.H.; Chen, D.Y.; Jiang, Y.; Mao, L.; Niu, J.L.; Zhang, J.; Yuan, G.Y. Biocompatibility of Mg–Nd–Zn–Zr Alloy with Rabbit Blood. *Chin. Sci. Bull.* **2013**, *58*, 2903–2908. [[CrossRef](#)]
185. Yu, W.; Chen, D.; Ding, Z.; Qiu, M.; Zhang, Z.; Shen, J.; Zhang, X.; Zhang, S.; He, Y.; Shi, Z. Synergistic Effect of a Biodegradable Mg–Zn Alloy on Osteogenic Activity and Anti-Biofilm Ability: An in Vitro and in Vivo Study. *RSC Adv.* **2016**, *6*, 45219–45230. [[CrossRef](#)]
186. Yu, W.; Zhao, H.; Ding, Z.; Zhang, Z.; Sun, B.; Shen, J.; Chen, S.; Zhang, B.; Yang, K.; Liu, M.; et al. In Vitro and in Vivo Evaluation of MgF₂ Coated AZ31 Magnesium Alloy Porous Scaffolds for Bone Regeneration. *Colloids Surf. B Biointerfaces* **2017**, *149*, 330–340. [[CrossRef](#)] [[PubMed](#)]
187. Miura, C.; Shimizu, Y.; Imai, Y.; Mukai, T.; Yamamoto, A.; Sano, Y.; Ikeo, N.; Isozaki, S.; Takahashi, T.; Oikawa, M.; et al. In Vivo Corrosion Behaviour of Magnesium Alloy in Association with Surrounding Tissue Response in Rats. *Biomed. Mater.* **2016**, *11*, 025001. [[CrossRef](#)]
188. Sato, T.; Shimizu, Y.; Odashima, K.; Sano, Y.; Yamamoto, A.; Mukai, T.; Ikeo, N.; Takahashi, T.; Kumamoto, H. In Vitro and in Vivo Analysis of the Biodegradable Behavior of a Magnesium Alloy for Biomedical Applications. *Dent. Mater. J.* **2019**, *38*, 11–21. [[CrossRef](#)]
189. Jiang, H.; Wang, J.; Chen, M.; Liu, D. Biological Activity Evaluation of Magnesium Fluoride Coated Mg–Zn–Zr Alloy in Vivo. *Mater. Sci. Eng. C* **2017**, *75*, 1068–1074. [[CrossRef](#)]
190. Zhang, N.; Liu, N.; Sun, C.; Zhu, J.; Wang, D.; Dai, Y.; Wu, Y.; Wang, Y.; Li, J.; Zhao, D.; et al. In Vivo Study of a Novel Micro-Arc Oxidation Coated Magnesium-Zinc-Calcium Alloy Scaffold/Autologous Bone Particles Repairing Critical Size Bone Defect in Rabbit. *Zhongguo Xiu Fu Chong Jian Wai Ke Za Zhi* **2018**, *32*, 298–305. [[CrossRef](#)]
191. Li, G.; Zhang, L.; Wang, L.; Yuan, G.; Dai, K.; Pei, J.; Hao, Y. Dual Modulation of Bone Formation and Resorption with Zoledronic Acid-Loaded Biodegradable Magnesium Alloy Implants Improves Osteoporotic Fracture Healing: An in Vitro and in Vivo Study. *Acta Biomater.* **2018**, *65*, 486–500. [[CrossRef](#)]
192. Xu, H.; Zhang, F.; Wang, H.; Geng, F.; Shao, M.; Xu, S.; Xia, X.; Ma, X.; Lu, F.; Jiang, J. Evaluation of a Porous Bioabsorbable Interbody Mg–Zn Alloy Cage in a Goat Cervical Spine Model. *BioMed Res. Int.* **2018**, *2018*, 7961509. [[CrossRef](#)]
193. Cihova, M.; Martinelli, E.; Schmutz, P.; Myrissa, A.; Schäublin, R.; Weinberg, A.M.; Uggowitzer, P.J.; Löffler, J.F. The Role of Zinc in the Biocorrosion Behavior of Resorbable Mg–Zn–Ca Alloys. *Acta Biomater.* **2019**, *100*, 398–414. [[CrossRef](#)] [[PubMed](#)]
194. Schaller, B.; Saulacic, N.; Beck, S.; Imwinkelried, T.; Liu, E.W.Y.; Nakahara, K.; Hofstetter, W.; Iizuka, T. Osteosynthesis of Partial Rib Osteotomy in a Miniature Pig Model Using Human Standard-Sized Magnesium Plate/Screw Systems: Effect of Cyclic Deformation on Implant Integrity and Bone Healing. *J. Cranio-Maxillofac. Surg.* **2017**, *45*, 862–871. [[CrossRef](#)] [[PubMed](#)]
195. Lin, Z.; Zhao, Y.; Chu, P.K.; Wang, L.; Pan, H.; Zheng, Y.; Wu, S.; Liu, X.; Cheung, K.M.C.; Wong, T.; et al. A Functionalized TiO₂/Mg₂TiO₄ Nano-Layer on Biodegradable Magnesium Implant Enables Superior Bone-Implant Integration and Bacterial Disinfection. *Biomaterials* **2019**, *219*, 119372. [[CrossRef](#)]
196. Marukawa, E.; Tamai, M.; Takahashi, Y.; Hatakeyama, I.; Sato, M.; Higuchi, Y.; Kakidachi, H.; Taniguchi, H.; Sakamoto, T.; Honda, J.; et al. Comparison of Magnesium Alloys and Poly-L-Lactide Screws as Degradable Implants in a Canine Fracture Model. *J. Biomed. Mater. Res. B Appl. Biomater.* **2016**, *104*, 1282–1289. [[CrossRef](#)]
197. Oshibe, N.; Marukawa, E.; Yoda, T.; Harada, H. Degradation and Interaction with Bone of Magnesium Alloy WE43 Implants: A Long-Term Follow-up in Vivo Rat Tibia Study. *J. Biomater. Appl.* **2019**, *33*, 1157–1167. [[CrossRef](#)]
198. Torroni, A.; Xiang, C.; Witek, L.; Rodriguez, E.D.; Flores, R.L.; Gupta, N.; Coelho, P.G. Histo-Morphologic Characteristics of Intra-Osseous Implants of WE43 Mg Alloys with and without Heat Treatment in an in Vivo Cranial Bone Sheep Model. *J. Cranio-Maxillofac. Surg.* **2018**, *46*, 473–478. [[CrossRef](#)] [[PubMed](#)]

199. Torroni, A.; Xiang, C.; Witek, L.; Rodriguez, E.D.; Coelho, P.G.; Gupta, N. Biocompatibility and Degradation Properties of WE43 Mg Alloys with and without Heat Treatment: In Vivo Evaluation and Comparison in a Cranial Bone Sheep Model. *J. Cranio-Maxillofac. Surg.* **2017**, *45*, 2075–2083. [[CrossRef](#)]
200. Niu, J.; Xiong, M.; Guan, X.; Zhang, J.; Huang, H.; Pei, J.; Yuan, G. The in Vivo Degradation and Bone-Implant Interface of Mg-Nd-Zn-Zr Alloy Screws: 18 Months Post-Operation Results. *Corros. Sci.* **2016**, *113*, 183–187. [[CrossRef](#)]
201. Bai, C.Y.; Li, J.W.; Ta, W.B.; Li, B.; Han, Y. In Vivo Study on the Corrosion Behavior of Magnesium Alloy Surface Treated with Micro-Arc Oxidation and Hydrothermal Deposition. *Orthop. Surg.* **2017**, *9*, 296–303. [[CrossRef](#)]
202. Plaass, C.; von Falck, C.; Ettinger, S.; Sonnow, L.; Calderone, F.; Weizbauer, A.; Reifenrath, J.; Claassen, L.; Waizy, H.; Daniilidis, K.; et al. Bioabsorbable Magnesium versus Standard Titanium Compression Screws for Fixation of Distal Metatarsal Osteotomies—3 Year Results of a Randomized Clinical Trial. *J. Orthop. Sci.* **2018**, *23*, 321–327. [[CrossRef](#)]
203. Helmecke, P.; Ezechieli, M.; Becher, C.; Köhler, J.; Denkena, B. Resorbable Interference Screws Made of Magnesium Based Alloy. *Biomed. Eng. Biomed. Tech.* **2013**, *58*, 000010151520134074. [[CrossRef](#)] [[PubMed](#)]